KINETIC STUDIES AND A COMPARISON OF ENZYME REGULATORY MECHANISMS IN *BLASTOCLADIELLA EMERSONII*

by

Glenn R. Klassen

A Thesis
Submitted to
the Faculty of Graduate Studies and Research
In Partial Fulfilment
of the Requirements for the Degree
Master of Science
1969

TO BETTY, PAUL AND ANDREA

ACKNOWLEDGEMENT

The author wishes to express sincere gratitude to Dr. H.B. LeJohn for his invaluable assistance and encouragement in this course of this investigation.

ABSTRACT

An $NADP^+$ specific isocitrate dehydrogenase and a glutamine synthetase were isolated from Blastocladiella emersonii and some of their kinetic and regulatory properties were studied. On the basis of product inhibition studies a Ping Pong Uni-Uni-Uni-Binary kinetic mechanism (Cleland, W.W., Biochim. Biophys. Acta, 67, 104, 1963) was proposed for the oxidative decarboxylation reaction of the $NADP^+$ specific isocitrate dehydrogenase. The reductive carboxylation reaction of the enzyme was observed to have cooperative kinetics. It was found that citrate acts as a negative effector in both directions of assay.

An extension of kinetic studies done on the NAD^+ specific isocitrate dehydrogenase from Blastocladiella (LeJohn, H.B., McCrea, B.E., Suzuki, I, and Jackson, Susan, J. Biol. Chem., 244, 9, 1969) revealed that NAD^+ and citrate could induce negative cooperative effects on the enzyme, and that anions could act as negative effectors on the enzyme.

Glutamine synthetase was found to be inhibited by a variety of metabolites and end-products including citrate and α-ketoglutarate. Inhibition by the amino acids, alanine, glycine and histidine showed antagonistic interactions between inhibitors, but inhibition by AMP and CTP was identified as cumulative feedback inhibition.

From these studies an attempt was made to develop a physiological scheme integrating what is known of the regulation of NAD^+ and $NADP^+$ specific isocitrate dehydrogenase, glutamate dehydrogenase and glutamine synthetase of Blastocladiella emersonii.

ABBREVIATIONS

α-KG	α-ketoglutarate
AMP	adenosine monophosphate
ADP	adenosine diphosphate
ATP	adenosine triphosphate
CTP	cytosine triphosphate
EDTA	(sodium) ethylenediamine tetra acetic acid
GMP	guanosine monophosphate
GTP	quanosine triphosphate
GDH	glutamate dehydrogenase
GAP	glucosamine 6-phosphate
IDH	isocitrate dehydrogenase
NAD^+	nicotinamide adenine dinucleotide (oxidized)
NADH	nicotinamide adenine dinucleotide (reduced)
$NADP^+$	nicotinamide adenine dinucleotide phosphate (oxidized)
NADPH	nicotinamide adenine dinucleotide phosphate (reduced)
tris	tris (hydroxymethyl)-aminomethane

TABLE OF CONTENTS

LIST OF FIGURES

LIST OF TABLES

INTRODUCTION

The advantages of using Blastocladiella emersonii as a model system for experimental studies of differentiation were discussed by Cantino and Lovett (1964). The organism can be maintained in large, single-generation, synchronized cultures, and its ontogeny can be easily directed along the OC (ordinary colourless) or the RS (resistant sporangial) pathway by simply withholding or adding bicarbonate to the growth medium. Ontogeny along either pathway proceeds in clearly recognizable stages which may be separately studied.

One approach to the problem of correlating the biochemistry of the organism with its morphogenesis is the study of enzyme regulation. This approach is advantageous in that the enzyme may be isolated at any stage in the life cycle, and yet its regulatory features may be correlated with physiological events at any other stage. This is possible if it is assumed that one protein does not change into another during physiological change, but that it may change in conformation, and hence in its activity.

It is known that certain molecules can act as triggers to initiate new steps in differentiation. As already stated, bicarbonate triggers RS development. The problem is to interpret these macroscopic effects in molecular terms, and to identify the level at which the trigger operates, whether at the level of the gene or at the level of enzyme modulation. Studies of enzyme induction and repression, (Khouw and McCurdy, 1969), as well as RNA synthesis, (Lovett, 1968), have shown that genetic controls are at work during differentiation, but whether these controls are elicited directly by molecular triggers or mediated by enzyme reactions is not known.

This study is an extention, on a number of fronts, of work on enzyme

modulation in B. emersonii. Its aim is to correlate enzyme controls with what is known about the control over differentiation by various nutrients, nucleotides, and ions. It is thought probable that at least some of the triggers may initiate change by a primary effect on enzyme activity rates at crucial branch points of the network of metabolic pathways. The sequence,

Isocitrate <——> α-ketoglutarate <——> glutamate <——> glutamine,

mediated by isocitrate dehydrogenase, glutamate dehydrogenase and glutamine synthetase respectively, is of crucial regulatory significance because it links the catabolic, energy-producing citric acid cycle with a complex network of biosynthetic reactions. The central enzyme in this scheme, glutamate dehydrogenase, has been studied intensely by LeJohn and his collaborators, (1968, 1969), and will be discussed in section III of the "Historical" part of this study. The following reports will concentrate on the two isocitrate dehydrogenases, particularly the one specific for the cofactor $NADP^+$, and on glutamine synthetase.

HISTORICAL

I. $NADP^+$-specific Isocitrate Dehydrogenase

$NADP^+$ specific IDH has been isolated from a wide variety of animals, plants, and microorganisms. Its occurence seems to be more general than that of the NAD^+-specific IDH, which is not normally found in bacteria. It was first found in porcine heart tissue, and the original definitive studies were done with this enzyme (Ochoa and Weisz-Tabori, 1945). These studies led to the proposal that the reaction proceeds as follows in the presence of Mn^{++} (Plaut, 1963):

$$\text{Isocitrate} + \text{enzyme} \rightleftharpoons \text{Isocitrate}\cdot\text{enzyme}$$

$$\text{Isocitrate}\cdot\text{enzyme} + NADP^+ \rightleftharpoons \text{Oxalosuccinate}\cdot\text{enzyme} + NADPH + H^+$$

$$\text{Oxalosuccinate}\cdot\text{enzyme} \rightleftharpoons \alpha\text{-ketoglutarate}\cdot\text{enzyme} + CO_2$$

$$\alpha\text{-ketoglutarate}\cdot\text{enzyme} \rightleftharpoons \alpha\text{-ketoglutarate} + \text{enzyme}$$

The molecular weight was estimated to be 61,000 by diffusion studies, (Moyle and Dixon, 1956), and the pH optimum was found to be 8.0. The pH curve was very broad compared with that for the NAD^+ specific IDH (Plaut and Sung, 1954). It was found that Mg^{++} could take the place of Mn^{++} as the cofactor, but with moderate loss of activity (Kornberg and Pricer, 1951).

In eucaryotes, it has been of interest to study the localization of the enzyme in the cell, relative to the localization of the NAD^+-specific IDH. Whereas the NAD^+-specific IDH is found exclusively within the mitochondria, (Plaut and Sung, 1954; Ernster and Navazio, 1956; Sung and Hsu, 1957), the $NADP^+$-specific IDH has been found both in the cytosol and the mitochondria, in different ratios. Early determinations found small amounts in mitochondria, and it was suspected that this simply represented

cytoplasmic contamination (Plaut and Sung, 1954). More recent reports, however, have established that the enzyme is present in the mitochondria of rat, pigeon, and locust, (Goebell and Klingenberg, 1964; Ernster and Navazio, 1957), and yeast (Bernofsky and Utter, 1966). It is probable that the distribution of the enzyme between cytosol and mitochondria varies from one tissue to another in the same organism. Rat brain cells are reported to have 65% of their enzyme in the mitochondria, (Salganicoff and Koeppe, 1968), whereas rat liver cells have only 10% in the mitochondria (Ernster and Navazio, 1957).

The presence of $NADP^+$-specific IDH in the mitochondria raises the question of its involvement in the citric acid cycle. Kaplan (1956) proposed, from studies on rat liver mitochondria, that mitochondrial oxidation of isocitrate was $NADP^+$ dependant, and that the NADPH formed was transferred to the electron transport chain by the transhydrogenase reaction:

$$NADPH + NAD^+ \rightleftharpoons NADP^+ + NADH$$

Purvis (1958) supported this formulation. Ernster and Navazio (1957), however, found that isocitrate could be oxidized both by an $NADP^+$ dependant route and an NAD^+ dependant route, and that the former was less effective that the latter. This result was confirmed when it was found that the NAD^+ specific enzyme is sensitive to allosteric control whereas no controls were found on the $NADP^+$ specific enzyme (Plaut and Chen, 1963). As more regulatory studies have been done on the NAD^+ specific enzyme from various sources, it has become clear that it is fully integrated into the citric acid cycle, and indeed, catalyses an important rate limiting step (Goebell and Klingenberg, 1964; Sanwal *et al*, 1965; Stein *et al*, 1967). This has left the question of the function of the $NADP^+$

specific IDH open.

The most obvious possibility is that the enzyme functions, inside or outside the mitochondria, in supplying NADPH for reductive biosynthesis (Greville, 1969). This enzyme and the glucose-6-P dehydrogenase appear to be the only sources of NADPH which the cell can draw on for fat synthesis.

There is evidence that the enzyme, when coupled with the transhydrogenase enzyme, is a bonafide alternative to the NAD^+ specific IDH for the complete oxidation of isocitrate (Stein, 1967). It is striking that tissues which have a high proportion of their $NADP^+$ specific IDH in the mitochondria also have high levels of transhydrogenase (Stein et al, 1959). This supports the idea that the $NADP^+$ route of isocitrate oxidation can be of respiratory significance, and suggests that the transhydrogenase reaction might control the activity of the $NADP^+$ specific IDH. Bernofsky and Utter (1968), have proposed that the $NADP^+$ specific IDH could be controlled by the levels of triphosphopyridine nucleotides in the mitochondria, which, in turn, is controlled by NAD^+ kinase.

Several recent reports indicate that the $NADP^+$ specific IDH from several species of bacteria and, significantly, from one protozoan, Crithidia fasciculata, may be modulated allosterically by nucleotides and by glyoxalate and oxaloacetate. (Shiio and Ozaki, 1967; Ozaki and Shiio, 1968; Marr and Weber, 1968, 1969; Hansen and MacKechnie, 1969). The nucleotide effect, inhibition by ATP, is explained on the basis of $NADP^+$ specific IDH involvement in oxidative metabolism by way of transhydrogenase (Marr and Weber, 1969). The inhibitory effect of glyoxalate and oxaloacetate is interpreted to mean that the onset of isocitrate lyase activity, brought about by low concentrations of intermediates, results in the inhibition of IDH activity by initial glyoxalate production. This switches the citric acid cycle off and allows intermediates to go into carbohydrate and fat metabolism. The fact that

bacteria have no mitochondria, and in general, no NAD^+ specific IDH, limits the importance of this work for general application to the problems discussed earlier.

II. Glutamine Synthetase

Glutamine synthesis in cell-free extracts from various animal tissues was first observed by Krebs and his collaborators (Krebs, 1935; Ostrom et al, 1939). Ten years later it was established that ATP and Mg^{++} were necessary for the reaction, with ATP being the source of energy. (Leuthardt and Bujard, 1947). Shortly thereafter, the complete reaction was formulated as follows:

$$\text{Glutamate} + NH_3 + ATP \overset{Mg^{++}}{\rightleftharpoons} \text{Glutamine} + ADP + P_i$$

(Speck, 1949; Elliott and Gale, 1948; Elliott, 1951)

Original enzyme preparations from animal tissues were purified 10 or 20 fold, but in 1953 Elliott purified the enzyme 1000 to 2000 fold from pea seed. This made possible the first physico-chemical studies of the enzyme. Recently, interest has shifted to the properties of the enzyme in microorganisms. The enzyme has been purified from Escherichia coli and obtained as a crystalline protein. (Woolfolk et al, 1966). Physico-chemical studies on this protein have subsequently yielded extraordinary results with respect to subunit structure, enzyme modification by another enzyme, and protein conformation (Valentine, Shapiro and Stadtman, 1968; Kingdon, Shapiro and Stadtman, 1967; Shapiro and Stadtman, 1967). The enzyme has also been isolated from a wide variety of microorganisms (Ravel et al, 1965; Kohlhaw et al, 1965; Hubbard and Stadtman, 1967).

This paper is primarily concerned with the regulation of glutamine synthetase by multiple end product inhibition. Woolfolk and Stadtman reported in 1964 that eight such inhibitors had been discovered for the E. coli enzyme, namely AMP, carbamyl phosphate, alanine, CTP, glycine, tryptophan, glucosa-

mine-6-phosphate, and histidine. If it is assumed that glutamine could have a role in amino acid synthesis by transamination with keto acids, all eight substances can be viewed as end products of the reaction catalysed by glutamine synthetase. It has also been found that glutamine, the immediate product, is also a potent inhibitor of the enzyme from Lactobacillus arabinosus (Ravel, 1965), Salmonella tryphimurium, Bacillus cereus, Bacillus lichenformis, Clostridium pasteurianum, and Rhododspirillum rubrum (Hubbard, 1967). For Saccharomyces cerevisiae, Kohlhaw has reported NAD^+ and GMP as additional inhibitors (1965).

Investigation of the interactions of the inhibitors with each other has resulted in the adoption of the term "cumulative feedback inhibition", (Rall and Sutherland, 1961), to describe what was found (Woolfolk and Stadtman, 1964, 1967). Cumulative feedback inhibition occurs when the "total residual enzyme activity in the presence of several inhibitors is equal to the product of the fractional activities observed when each of the inhibitors is tested alone" (Woolfolk and Stadtman, 1967). This type of inhibition would occur if each inhibitor had its own inhibition site on the enzyme. If more than one enzyme was being inhibited, the result would be additive inhibition. If the inhibitors were competing for the same allosteric site, total inhibition by several inhibitors should not exceed the effect of the most potent inhibitor in the mixture. Both of these latter possibilities have been eliminated by exhaustive pairing of inhibitors and by experiments in which as many as eight inhibitors were present simultaneously (Woolfolk and Stadtman, 1964, 1967). The specificity of each site was further confirmed by experiments with analogs of the inhibitors. It was found that L-serine is also an effective inhibitor, but only at the alanine site (Woolfolk and Stadtman, 1967). Sigmoidal plots

for alanine suggest that there may be two inhibitor sites for each of these molecules (Woolfolk and Stadtman, 1967).

Studies with glutamine synthetase from B. lichenformis, in contrast to those done with E. coli, show substantial interactions between inhibitors involving both synergism and antagonism. On the basis of the data, five distinct inhibitor sites are proposed, with AMP playing the role of key inhibitor (Hubbard and Stadtman, 1967).

Cumulative feedback inhibition is presumed to operate on glutamine synthetase activity in precise proportion to the amount of glutamine needed to supply the end product which is inhibiting. This type of control, in all its complexity and elegance, and with the suggestion that it may appear in infinite variety in different organisms, should lend itself well to the development of a unified view of cellular control, enzyme adaptation, and evolution.

III. Enzyme Regulation in B. emersonii

The study of enzyme regulation in B. emersonii is in its infancy. Detailed kinetic and physical studies have been done only with an NAD^+ specific glutamate dehydrogenase and an NAD^+ specific isocitrate dehydrogenase (LeJohn and Jackson, 1968; LeJohn, 1968a,b, LeJohn et al, 1969a,b). Preliminary kinetic studies have been done on malate dehydrogenase and glucose-6-P dehydrogenase (LeJohn, unpublished data).

Glutamate dehydrogenase has been purified over 100 fold and shown to be "regulatory" by all criteria. It shows sigmoidal dependance of velocity on substrate concentration (LeJohn and Jackson, 1968a), allosteric interactions between the enzyme and certain effectors (LeJohn and Jackson, 1968a; LeJohn, 1968a,b), is subject to densitization by Hg^{++} at allosteric sites (LeJohn and Jackson, 1968b), and has been shown to be polymeric

(LeJohn and Jackson, 1968a). It is mitochondrial and its molecular weight has been estimated as 230,000 ± 20,000 daltons (LeJohn and Jackson, 1968a).

The enzyme is sensitive to modulation by nucleotides, protons, metabolites and metal ions. It may be activated 8 fold by AMP or ADP and inhibited by about the same factor by ATP or GTP. It was shown that the optimum pH shifts from 8.0 to 10.0 with increasing activation by effectors. At pH 6.0 the enzyme is still active, but insensitive to modulation. The metabolites citrate, isocitrate, fructose 1,6 diphosphate, fumarate, and α-ketoglutarate were found to inhibit only the oxidative deamination of glutamate, and this rare mechanism was called "unidirectional inhibition" (LeJohn, 1968a). Experiments with metal ions showed a 3 fold activation of the reductive amination of α-ketoglutarate by Ca^{++} and Mn^{++}, but inhibition of the oxidative deamination of glutamate by Ca^{++} (LeJohn, 1968b). Increasing pH enhances both effects.

The NAD^{+} specific IDH has been purified 450 fold and has been shown to have complex regulatory features (LeJohn, McCrea, Suzuki, and Jackson, 1969). AMP and citrate are allosteric activators of a virtually irreversible oxidation of isocitrate. In the presence of either AMP or citrate, the kinetic mechanism was found to be ordered binary-ternary, according to the terminology of Cleland (1963). The effect of protons in the modulation of IDH, as in the case of GDH, was synergistic with respect to the other effectors. Specifically, pH curves were complex in the presence of low concentrations of activators, showing two optima, one at pH 6.5 and the other at pH 9.0. This was interpreted to mean that pH effects operated on two ionic equilibria. In the acid region, OH^{-} and citrate act in concert to transform an inactive

polymer into an active monomer. In the alkaline region, OH^- and AMP or citrate act together to transform the acid monomer to an active alkaline monomer.

Since both enzymes are mitochondrial, and since the product of isocitrate oxidation, α-ketoglutarate, is a substrate for the reductive amination reaction of glutamate dehydrogenase, it was proposed that the enzymes are coupled in the mitochondria, with glutamate dehydrogenase on the outer surface of the organelle and isocitrate dehydrogenase inside (LeJohn et al, 1969a). On this basis, the controls on the enzymes were correlated and a probable physiological role suggested for their concerted action.

Two sets of conditions were visualized; a) The mitochondria were said to be "energized" when citric acid cycle intermediates are abundant, energy production is intense, and cations are being translocated into the mitochondria as H^+ are being expelled; b) The "unenergized" state was taken to be opposite in every respect.

In the energized state the intramitochondrial pH would be increasing as the extramitochondrial pH decreases. The result would be an activation of IDH and a corresponding inhibition of the oxidative deamination reaction of GDH. These effects would be reinforced by citrate and AMP modulation. Accumulation of citrate, together with increasing pH, would activate the IDH and inhibit the oxidative deamination of glutamate. The AMP-ATP ratio would be high due to high energy requirements, resulting in AMP activation of IDH and inhibition of the oxidative deamination of glutamate. Under these conditions, then, the coupled enzyme system would work to produce energy, and, at the same time, conserve valuable organic acids in a glutamate "sink" (LeJohn, 1968b). In the unenergized state, the controls

would be reversed, allowing glutamate to enter the citric acid cycle to supply intermediates.

The ultimate purpose of these investigations was to explain differentiation in B. emersonii. In these studies, the changes occuring during spore germination were of special interest. It is known that germination timing and competence depends on the environment of the spore. Starvation delays differentiation, and, if carried out for several hours, severely impairs viability (Cantino and Lovett, 1964). This suggests that small substrate molecules play a role in control of differentiation. Ca^{++}, EDTA, or citrate inhibit germination and Mn^{++}, Mg^{++}, and K^{+} can activate germination (Cantino et al, 1968). The effects of citrate and Ca^{++} have been tentatively correlated with enzyme controls. The zoospore has high energy requirements for motility. If its mitochondrion is in the energized state, as discussed above, this requirement could be met. The inhibition of germination by citrate and Ca^{++} would then correlate perfectly with their roles in modulating IDH and GDH as described above. This leads to the tentative conclusion that the timing of the onset of germination depends on the energy balance in the zoospore and may be influenced by the presence or absence of cations.

IV. Theories of Enzyme Regulation

The central problem in the field of enzyme regulation is to explain the cause and effect of cooperativity. Cooperativity occurs when "...at least two molecules of substrate interact with the enzyme and ... the binding of one molecule in some manner facilitates the binding of the next." (Stadtman, 1966). The sigmoid curves that this interaction generates

when enzyme velocity is plotted against substrate concentration were first observed with hemoglobin (Bohr, 1903; Adair, 1925), but the physiological significance was not fully appreciated until the present decade. Changeux (1963), pointed out that an enzyme showing cooperativity is sensitive to change in substrate concentration over a very narrow range and proposed that this amounts to a threshold effect by which the enzyme may be very delicately controlled. Subsequently, cooperativity has become the hallmark of regulatory enzymes.

Though there is unanimity on the effect of cooperativity, its physical interpretation is still controversial. Monod, Wyman and Changeux (1965), offered the first major formulation. They proposed that two or more conformationnal states of the enzyme (R and T), in equilibrium with each other, bind the substrate differentially. Multiple identical binding sites on each enzyme molecule, made possible by the aggregation of identical "protomers" into one "oligomer" result in the proliferation of a number of different enzyme-ligand associations for each conformational state (R_1, $R_2 \ldots R_n$ and T_1, $T_2 \ldots T_n$). They were able to show mathematically that when the affinity of the R state for the substrate is greater than the affinity of the T state, enzyme available for conformational transition, (Ro and To), decreases faster on the R side of the equilibrium, with the result that To is converted to Ro to maintain equilibrium conditions. Since R is more active than T, this results in a sudden accelleration of net enzyme velocity and is manifested as sigmoidicity in plots of kinetic data.

An important corollary of this formulation is that if the oligomer is to oscillate between two or more different conformations and still keep multiple identical sites in each, it should maintain its symmetry

under all conditions. As a result this model has come to be known as the symmetry model (Koshland et al, 1968). The symmetry requirement means that interprotomer bonds are so strong that an effect on one subunit results in a simultaneous and equal conformational change in all subunits. It also means that the nature of interactions after the first substrate binds does not change with successive bindings, since the first binding commits the entire molecule to the active conformation.

In 1966, Koshland, Nemethy and Filmer proposed an alternative model which has become known as the sequential model, because in it the conformational transition is not simultaneous for all subunits but may proceed protomer by protomer. The resulting hybrid conformational states lead to much more complex formulations, but the model is more flexible in that it allows the assumption of varying strengths of protomer interactions, and dispenses with the symmetry requirement. Thus, according to this model, the first binding does not determine the nature of subsequent bindings. This is tantamount to saying that the nature of interaction could change over a range of substrate concentration. Successive bindings could be either easier than the first or more difficult.

Experimental evidence to show that this could actually happen appeared from studies of the binding of NAD^+ to glyceraldehyde-3-P dehydrogenase from rabbit muscle (Koshland et al, 1968). These studies have shown that one molecule of NAD^+ binds to each tetramer of the enzyme before the second binds to any tetramer. Binding constants for all four NAD^+ molecules were evaluated and found to decrease dramatically from first to last, far beyond the values predicted by statistical calculations which assume that interaction does not change over the range of substrate concentration. The term "negative homotropic effect" was adopted to describe this

phenomenon (Koshland et al, 1968).

Monod et al (1965) anticipated the discovery of allosteric inhibition of an enzyme by excess substrate. They argued that their model could explain this when it is assumed that the conformational state with the higher affinity for substrate is catalytically inactive. It should also be remembered that their model does not exclude the existence of more than two conformational states.

Koshland et al (1968) take these results as a virtual confirmation of the sequential model for this enzyme. The binding constants obtained strongly suggest that the subunits change conformation relatively independently and the negative cooperative pattern obtained, even in the presence of unsaturating levels of substrate, cast doubt on the "all or nothing" conformational change proposed by the symmetry model.

MATERIALS AND METHODS

I. Preparation of Cells

The enzymes were isolated from a solid cake of zoosporangial Blastocladiella emersonii cells grown and prepared by the following procedure.

A single-generation, synchronized culture of B. emersonii was maintained on plates of Cantino agar* by daily transfer. Large masses of cells were grown in 10 liter carboys of liquid peptone-yeast-glucose medium containing 10^{-3} M phosphate buffer, pH 7.0, and 10 drops of Antifoam A. The zoospore inoculum for one carboys was prepared by inoculating 15 to 20 Roux bottles containing 125 ml of Cantino Agar with a suspension of zoospores grown on petri plates. The Roux bottles were incubated at 22° C for 20 hrs, and sporulation was induced by the addition of 15 ml of sterile water. After 30 mins the spores were harvested and introduced into the carboys aseptically. Flooding and harvesting was repeated two or three times for maximum yield of spores. The carboys were vigorously aerated during 16 hrs of incubation at 20°C. Cells were collected by suction filtration through Whatman #1 filter paper. The mat of cells was washed with phosphate buffer, pH 7.0, and partially dried by suction. Normally, extraction of the enzymes followed immediately upon collection of the cells, but occasionally the mat of cells was frozen and stored at -20°C.

---

* Cantino agar consists of 1.25 g yeast extract, 1.25 g bacteriological peptone, 3.0 g glucose per liter with 2% bactoagar.

II. Extraction, Purification and Storage of $NADP^+$ specific IDH

The cells were suspended in a buffer containing 0.05 M Tris-acetate, 0.05 M potasium phosphate buffer, pH 7.0, 10^{-4} M EDTA, 10^{-2} M Mg^{++}, and 10^{-4} Cleland's Reagent (Dithiothreitol). The suspension was sonicated in a Raytheon ultrasonicator in 25 ml batches for 10 mins each, and subsequently centrifuged at 27,000 x g for 10 mins. The supernatant fluid was then decanted and purified further as follows.

Step I. Acetone, prechilled to -20°C, was added slowly, dropwise, to the crude extract, which was under constant stirring. When the concentration of acetone reached 40%, the precipitate was separated by centrifugation at 27,000 x g for 10 mins.

Step II. More acetone was added to the supernatant from Step I until the concentration reached 60%. After centrifugation at 27,000 x g for 10 mins the supernatant fluid was discarded and the precipitate dried in a stream of air.

Step III. The precipitate was then suspended in a small volume of 30% ammonium sulphate in 0.05 M phosphate buffer, pH 7.0. The suspension was centrifuged at 12,000 x g for 5 mins, and the precipitate discarded. The supernatant was then brought to 10% in glycerol.

Step IV. A 40 x 2.5 cm column packed with Sephadex G-200 was washed with the suspending buffer mentioned above in 10% glycerol. The supernatant from Step III was adsorbed to the column and eluted with the suspending buffer. 4 ml fractions were collected automatically. Fractions containing significant enzyme activity were pooled.

The partially purified enzyme was suspended in 50% glycerol, frozen quickly and stored at -50°C.

III. Extraction, Purification and Storage of Glutamine Synthetase.

The cells were suspended in a buffer containing 10^{-2} M Imidazole and 10^{-2} M Mn^{++}, at pH 7.1. The suspension was sonicated in a Raytheon ultrasonicator in 50 ml batches for 30 mins each. The supernatant fluid was recovered by centrifugation at 27,000 x g for 15 mins. Further purification of the crude extract proceeded as follows.

Step I. The crude extract was brought to 35% saturation with ammonium sulphate. After stirring for one-half hour, the supernatant was recovered by centrifugation at 27,000 x g for 15 mins.

Step II. The supernatant was then brought to 60% saturation with ammonium sulphate and similarly centrifuged. The supernatant was discarded.

Step III. The precipitate from Step III was dissolved in a small volume of buffer and triturated for one-half hour in the cold. Then the suspension was rapidly brought to 50°C and kept at this temperature for 5 mins in a water bath. The suspension was then chilled and centrifuged at 48,000 x g for 10 mins.

Step IV. The supernatant was then dialysed against 100 volumes of buffer containing 10^{-2} M Imidazole, 10^{-2}M Mn^{++}, 10^{-4} M ATP, and 10^{-3} M glutamate, pH 7.1, for one hour. A further centrifugation removed precipitate.

The enzyme preparation was stored for short periods of time in the

frozen state.

IV. Enzyme Assays

Isocitrate Dehydrogenase

Kinetic assays, as well as assays used during purification of the enzymes, were done by measuring the rate of NAD^+ or $NADP^+$ reduction at 340 mμ on a model 2000 Gilford recording spectrophotometer. Mg^{++} was used routinely in the purification procedure due to the danger of precipitation with Mn^{++}, but for kinetic studies both metal ions were used as indicated in the figure legends. When Mn^{++} was used it was always added after mixing the substrates with the buffer to avoid local precipitation. Other reagents were used in concentrations reported with the experimental results. The total volume per assay was 3.0 ml using cuvettes of 10 mm light path. The unit of activity was defined as the concentration of enzyme which caused an O.D. change at 340 mμ of 0.001 per minute. Specific activity was expressed as units of activity per mg of protein. The method of Lowry et al (1951) was used for protein determination.

Glutamine Synthetase

The activity of glutamine synthetase was measured by colorimetric estimation of hydroxamate concentration in the reaction mixture after incubation with the enzyme.

$$\text{Glutamine} + \text{hydroxylamine} + \text{ATP} \rightleftharpoons \gamma\text{-glutamylhydroxamate} + NH_3 + \text{ADP} + P_i$$

The following standard conditions were used. Sufficient enzyme to give 300 µM or less of hydroxamate in 20 mins at 30°C was added to a total volume of 5 ml containing 100 mM glutamate, 2.5 mM Cleland's Reagent, 2.5 mM ATP, 100 mM hydroxylamine, 25 mM $MnCl_2$, and 25 mM Imidazole-HCl buffer to a final pH of 7.1. After incubation, the reaction was stopped and the color developed by the addition of one ml of a solution containing equal volumes of 25% TCA, 6 N HCl, and 10% $FeCl_3$ $3H_2O$ in 0.02 N HCl. After addition of the $FeCl_3$ reagent, the tubes were centrifuged at 15,000 x g for 5 mins and the optical density of the solution was measured with a Klett-Summerson colorimeter using a filter which transmits light in the 500 to 570 mµ range. Glutamine synthetase activity is expressed in terms of moles of hydroxamate formed, as determined by reference to a standard curve obtained with authentic γ-glutamylhydroxamate. For kinetic studies concentrations of reagents appear in the tables and figure legends.

CHEMICALS

The chemicals used were obtained from Sigma Chemical Company, St. Louis, Missouri.

RESULTS

I. $NADP^+$ specific Isocitrate Dehydrogenase

A. Purification

Table I records purification data for $NADP^+$ specific IDH. The 60 fold purified enzyme preparation was clear and colorless.

B. Kinetic Studies

Kinetic studies on $NADP^+$ specific isocitrate dehydrogenase were done with two aims in mind, namely; 1) to arrive at a probable kinetic mechanism for the reaction, and 2) to elucidate any control features it may have. The kinetic mechanism that will be proposed is based on initial velocity and product inhibition studies carried out on the oxidative decarboxylation reaction of the enzyme. The overall reaction can be represented as follows:

$$NADP^+ + \text{isocitrate} \xrightleftharpoons{Mn^{++} \text{or } Mg^{++}} NADPH + H^+ + \alpha\text{-ketoglutarate} + CO_2$$

(Plaut, 1963)

All kinetic data is presented in the double reciprocal form according to the method of Lineweaver and Burk (1934), the reciprocal of the velocity being plotted against the reciprocal of the substrate concentration. The conventions of Cleland (1963) are used in describing all results.

pH and Cofactor Requirements

It was found that the enzyme shows maximal activity between pH 8.0 and 9.0 (Fig. 1). This broad pH optimum indicates that the enzyme,

TABLE I

Purification of $NADP^+$ specific Isocitrate Dehydrogenase from *Blastocladiella emersonii*

Fraction	Total Protein (mg)	Total Activity (units)	Specific Activity (units/mg)	Purification (fold)	Recovery (percent)
Crude	925	250,000	270	-	100
40% Acetone supernatant	281	175,000	620	2.5	70
60% Acetone precipitate	36	156,000	4,330	16	62
G-200 Sephadex eluate	8	135,000	17,000	63	54

Fig. 1. The influence of pH on the maximal velocity of $NADP^+$ specific isocitrate dehydrogenase from Blastocladiella emersonii. The reaction system contained 66.67 mM tris-acetate buffer at the pH indicated, 0.33 mM $NADP^+$, 1.67 mM Mg^{++}, and 20 µg enzyme protein.

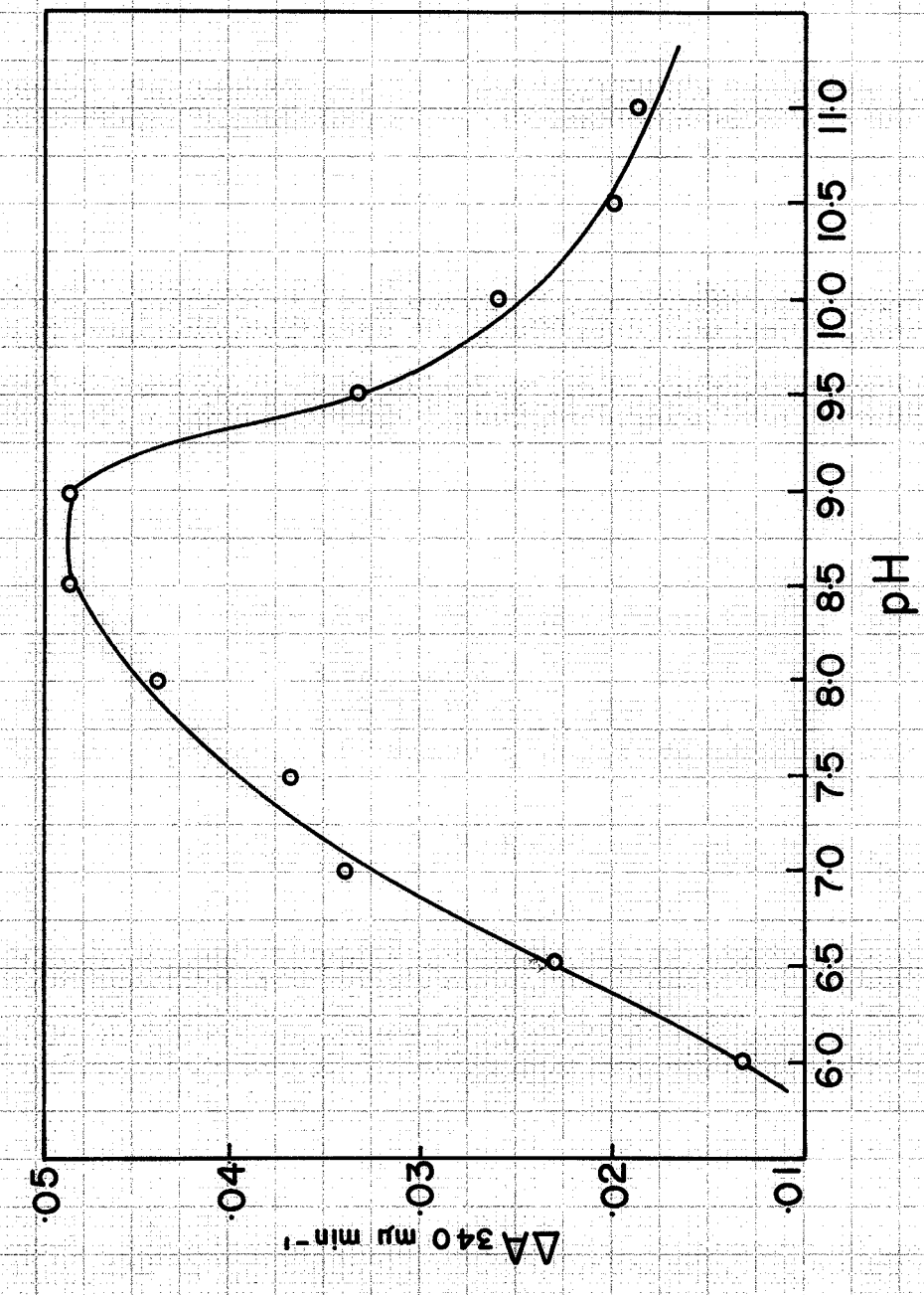
ΔA 340 mμ min⁻¹
.05
.04
.03
.02
.01
6.0
6.5
7.0
7.5
8.0
8.5
9.0
9.5
10.0
10.5
11.0
pH

unlike the NAD^+ specific IDH from Blastocladiella (McCrea, thesis), is relatively insensitive to small pH changes. Most kinetic studies were done at pH 8.0, but when bicarbonate was used as part of the reaction system, pH 8.5 was used to avoid loss of carbon dioxide from the reaction solution.

The reaction requires either Mn^{++} or Mg^{++} as a cofactor. Fig. 2 shows the relationship between cofactor concentration and enzyme velocity. The following observations may be made; 1) The approximate $S_{0.5}$ values for Mn^{++} and Mg^{++} are 0.3 mM and 0.2 mM respectively. The $S_{0.5}$ value is defined as the substrate (cofactor) concentration which yields one-half the maximal velocity (Vmax). Vmax is defined as the initial velocity under optimal conditions of substrate saturation. 2) The Vmax of the reaction with Mg^{++} as cofactor is approximately 70% of that with Mn^{++}; 3) The relationship between enzyme velocity and cofactor concentration appears to be sigmoidal in the rate-concentration plot.

Initial Velocity Studies

Experiments were done to determine the effect on the velocity of the enzyme when one substrate, designated the variable substrate was varied while the other substrate, designated the fixed substrate was held at a constant concentration. In each such experiment a number of concentrations of fixed substrate were chosen so that a set of curves was obtained. Replots of the intercepts versus the reciprocals of the concentrations of the fixed substrate were then used to find the Michaelis constants of the substrates (Florini and Vestling, 1957).

Fig. 2. Rate concentration plots of the effect of Mg^{++} and Mn^{++} on the maximal velocity of $NADP^{+}$ specific isocitrate dehydrogenase from B. emersonii. The reaction mixture contained 66.67 mM tris-acetate buffer, pH 8.0, 1.33 mM isocitrate, 0.33 mM $NADP^{+}$ and Mg^{++} and Mn^{++} as indicated, and 20 µg of enzyme protein.

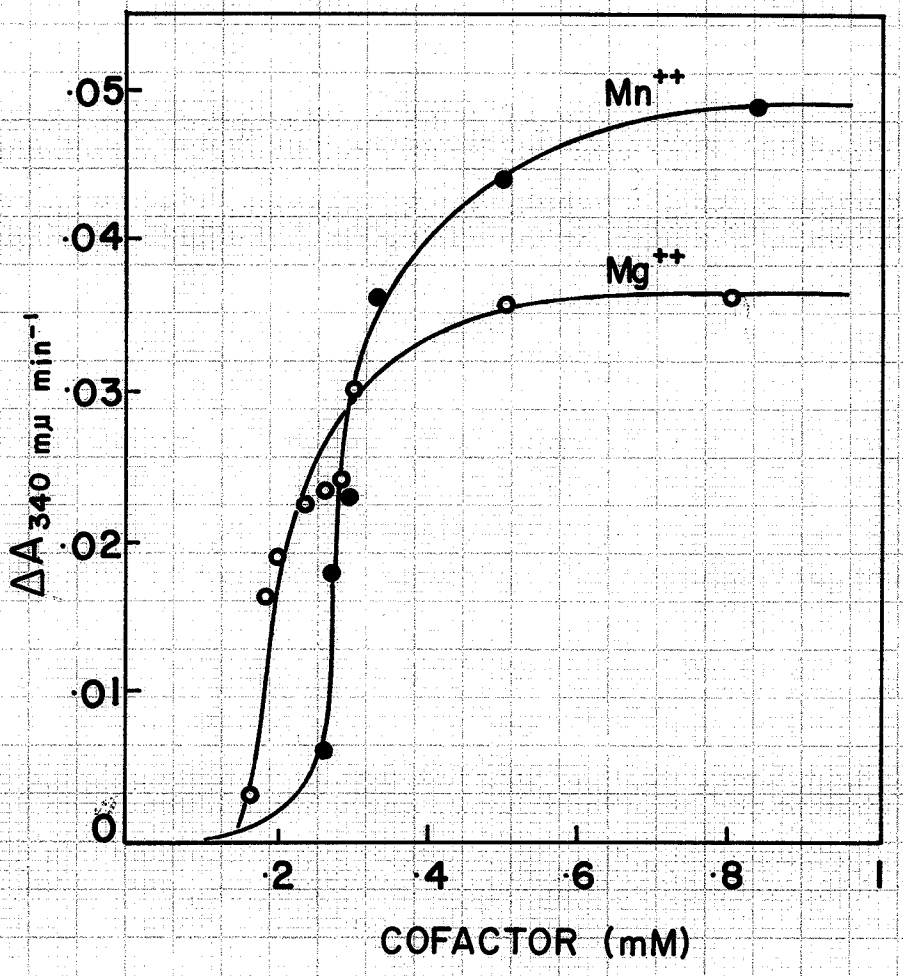
·05
·04
·03
·02
·01
0
ΔA_{340} mμ min^{-1}
Mn^{++}
Mg^{++}
·2
·4
·6
·8
1
COFACTOR (mM)

1. Isocitrate : $NADP^+$

When isocitrate was the variable substrate and $NADP^+$ the fixed substrate, a set of parallel lines was obtained (Fig. 3). A replot of the intercepts versus the reciprocal of $NADP^+$ concentration was linear (Fig. 3b). From Fig. 3 the K_m for $NADP^+$ was determined to be 6.6 μM.

2. $NADP^+$: Isocitrate

A set of parallel lines was also obtained with $NADP^+$ as the variable substrate and isocitrate as the fixed substrate (Fig. 4). The intercept replot is linear (Fig. 4b), and the Km for isocitrate, as determined from Fig. 4b is 15 μM.

Product Inhibition Studies

Initial velocities were studied in the presence of different fixed concentrations of one of the three products, α-ketoglutarate, NADPH, and carbon dioxide. Bicarbonate was used as a source of carbon dioxide. The nomenclature of Cleland (1963b) was used to describe the type of inhibition observed in each case. When only the slope of the set of lines obtained changes, the inhibition will be called competitive with respect to the variable substrate. When only the intercept changes, it will be called uncompetitive, and when both intercepts and slopes are different, it will be called noncompetitive. Inhibition constants are obtained by replotting either the intercepts or the slopes against inhibitor concentrations.

Unless otherwise stated, the fixed substrates were held at saturating levels, 0.166 mM of $NADP^+$ and 0.33 mM of isocitrate.

1. $NADP^+$: NADPH

NADPH inhibition when $NADP^+$ was the variable substrate appears

Fig. 3. Initial Velocity Studies.

(a) Double reciprocal plots of rate against isocitrate concentration. Reaction mixture contained 66.67 mM tris-acetate buffer, pH 8.0, 1.67 mM Mg^{++}, isocitrate and $NADP^{+}$ as indicated and 20 μg of enzyme protein.

(b) Replot of intercepts against reciprocals of $NADP^{+}$ concentrations for determination of K_m for $NADP^{+}$.

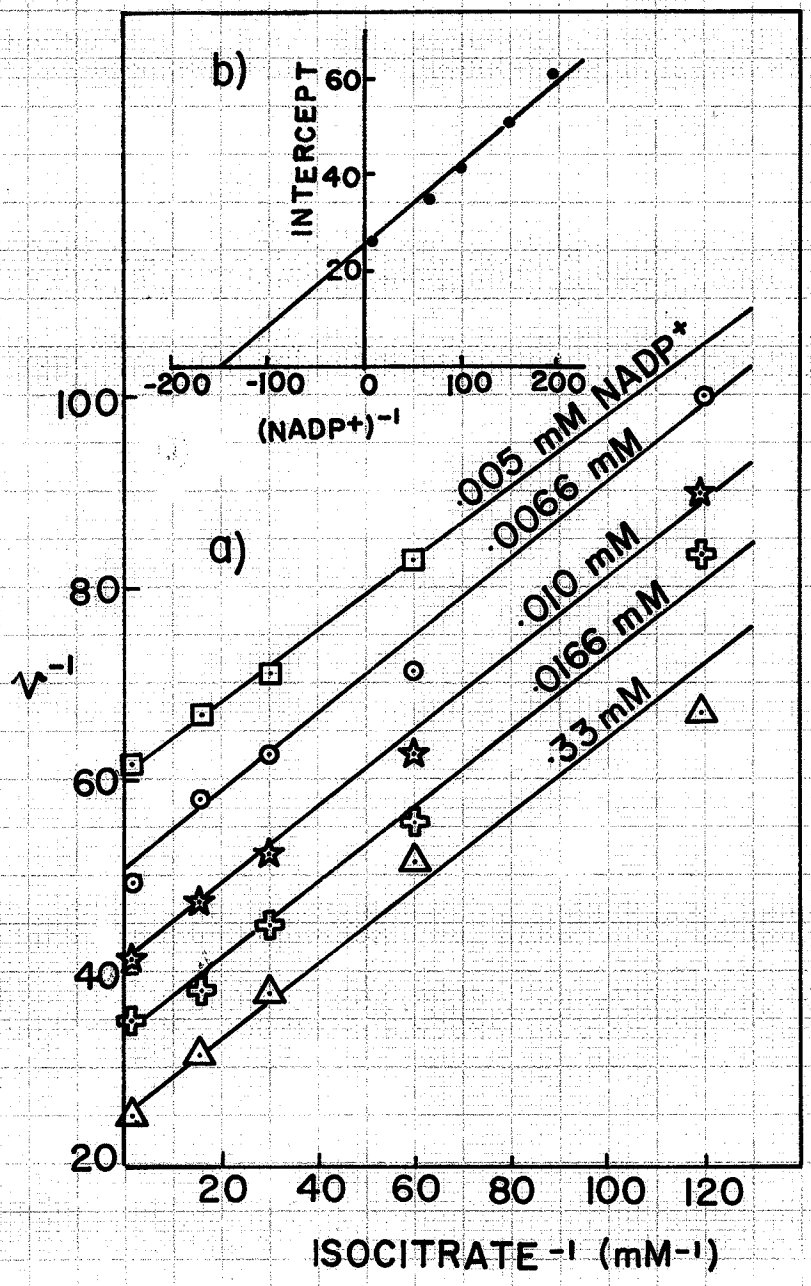
b)
INTERCEPT
60
40
20
-200
-100
0
100
200
(NADP+)⁻¹
a)
.005 mM NADP+
.0066 mM
.010 mM
.0166 mM
.33mM
v⁻¹
100
80
60
40
20
20
40
60
80
100
120
ISOCITRATE⁻¹ (mM⁻¹)

Fig. 4. Initial Velocity Studies

(a) Double reciprocal plots of velocity against $NADP^+$ concentration. The reaction system contained 66.67 mM tris-acetate buffer, pH 8.0, 1.67 mM Mg^{++}, isocitrate and $NADP^+$ as indicated, and 20 µg of enzyme protein.

(b) Replot of intercepts against reciprocals of isocitrate concentrations for determining the K_m for isocitrate.

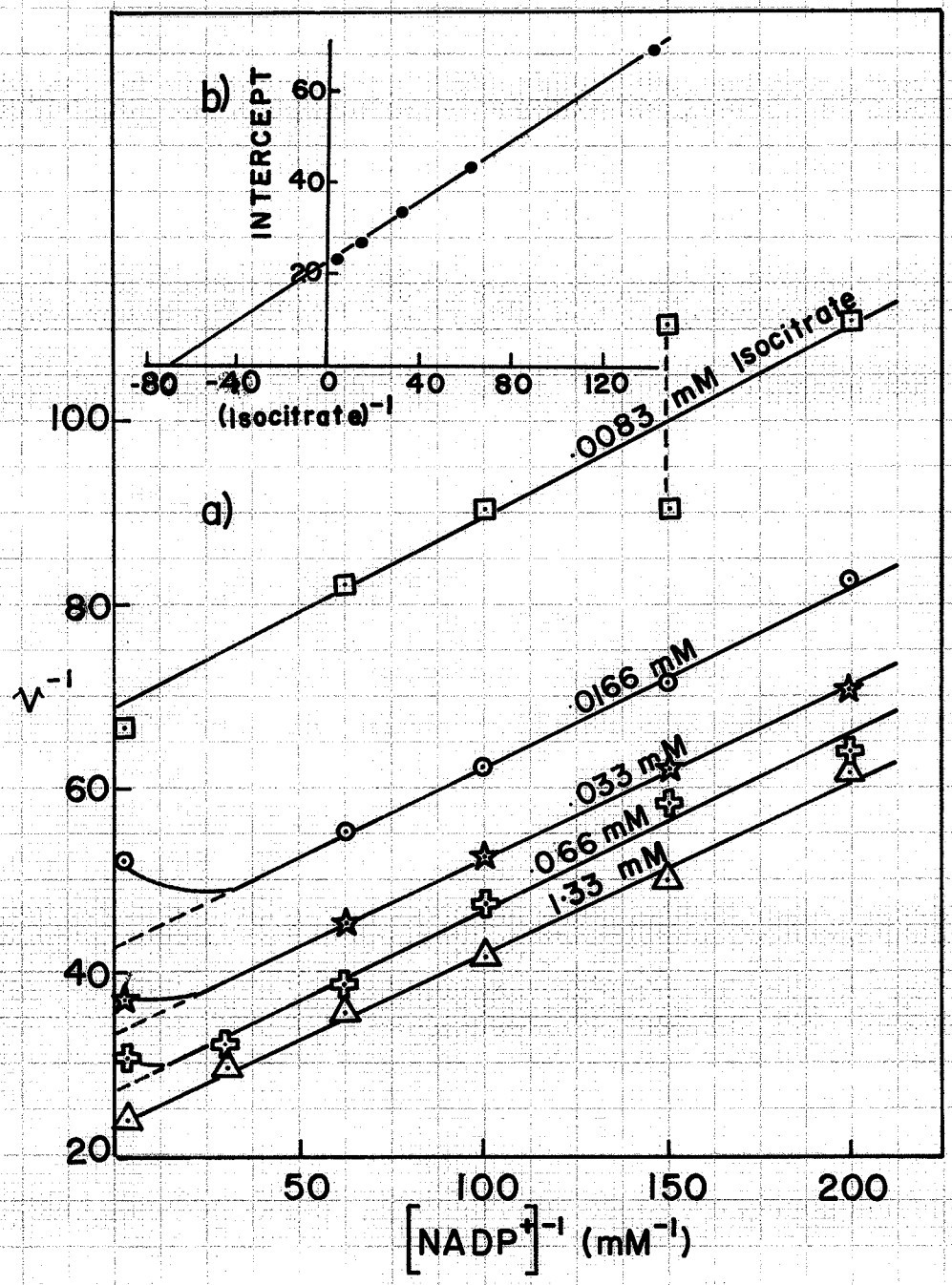
b)
INTERCEPT
60
40
20
-80
-40
0
40
80
120
(Isocitrate)$^{-1}$
a)
.0083 mM Isocitrate
0166 mM
.033 mM
066 mM
1·33 mM
v^{-1}
100
80
60
40
20
50
100
150
200
$[NADP^+]^{-1}$ (mM^{-1})

to be competitive (Fig. 5). The slope replot (Fig. 5b), is linear and yields an inhibition constant (K_i) of 21 μM. At high NADPH concentration (50 μM) the slope of the double reciprocal plot is disproportionately high, indicating that the inhibition pattern has changed in some way.

2. Isocitrate : α-ketoglutarate

With isocitrate as the variable substrate and α-ketoglutarate as the inhibitor, a competitive pattern was observed (Fig. 6). The slope replot (Fig. 6b) is linear and the K_i for α-ketoglutarate is 0.45 mM.

3. $NADP^+$: α-ketoglutarate

When $NADP^+$ was the variable substrate and α-ketoglutarate the inhibitor, preliminary studies showed that extremely high concentrations of α-ketoglutarate had to be used to obtain any significant inhibition. When the concentration of isocitrate, the fixed substrate, was reduced to unsaturating levels, 0.10 mM, inhibition of the uncompetitive type was observed with inhibitor concentration in the 1.66 mM to 5 mM range (Fig. 7). A replot of the intercepts is linear (Fig. 7b). Table II shows that with increasing isocitrate saturation, α-ketoglutarate inhibition approaches no inhibition.

4. Isocitrate : NADPH

With isocitrate as the variable substrate and NADPH as the inhibitor, high concentrations of NADPH yield an uncompetitive pattern (Fig. 8), whose replot is linear (Fig. 8b). When the $NADP^+$ concentration is increased beyond normal saturation (0.5 mM), no inhibition is observed

Fig. 5a) Product inhibition by NADPH on the reduction of $NADP^+$ catalysed by $NADP^+$ specific isocitrate dehydrogenase from Blastocladiella emersonii. The reaction mixture contained 66.67 mM tris-acetate buffer, pH 8.0, 1.67 mM Mg^{++}, 0.33 mM isocitrate, 20 µg enzyme protein, and $NADP^+$ and NADPH as indicated.

5b) Replot of the slopes against inhibitor concentrations.

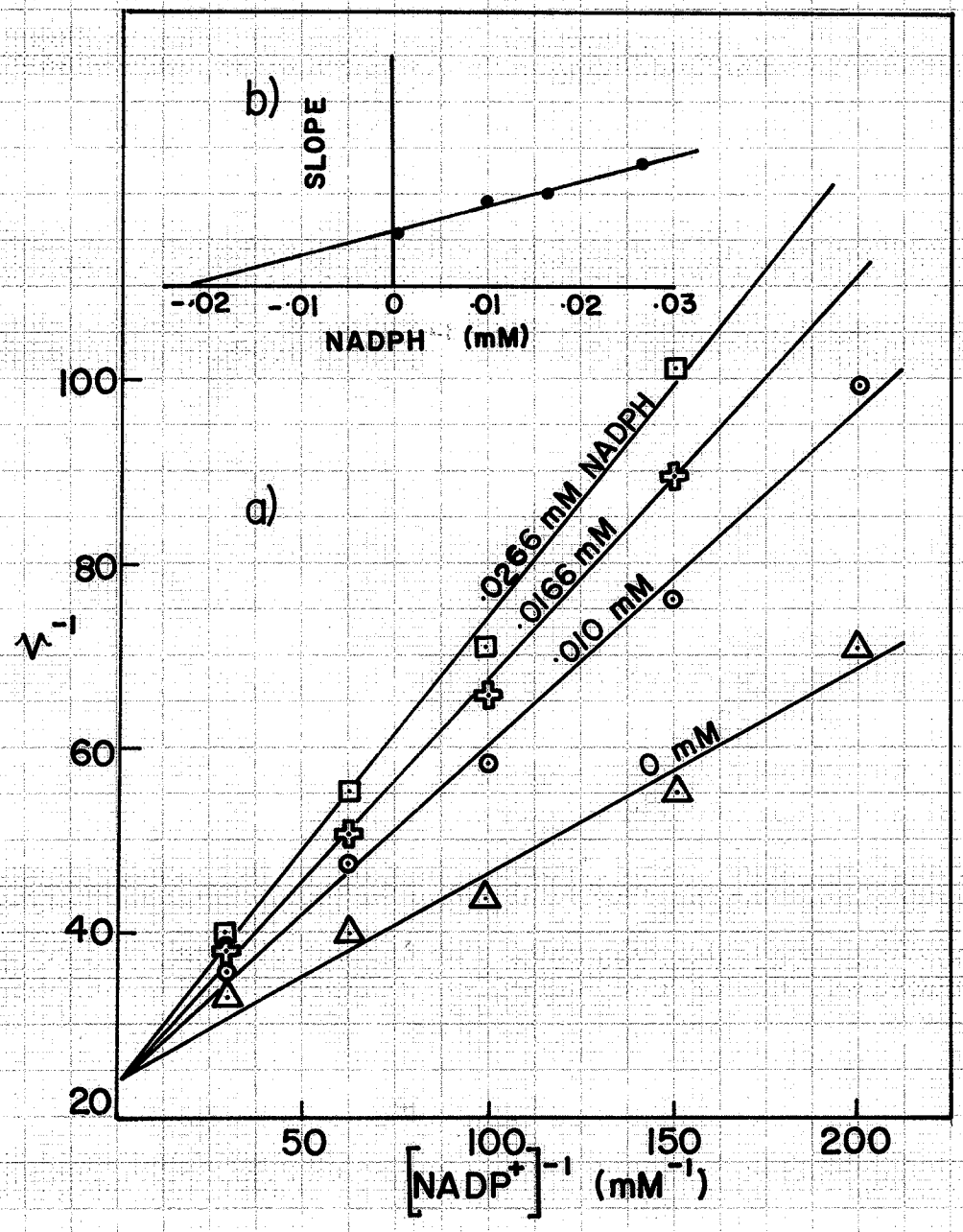
b)
SLOPE
-·02
-·01
0
·01
·02
·03
NADPH (mM)
a)
·0266 mM NADPH
·0166 mM
·010 mM
0 mM
v⁻¹
100
80
60
40
20
50
100
150
200
[NADP⁺]⁻¹ (mM⁻¹)

Fig. 6a) Product inhibition of α-ketoglutarate on the rate of decarboxylation of isocitrate by $NADP^+$ sp. isocitrate dehydrogenase from B. emersonii. The reaction system contained 66.67 mM tris-acetate buffer, pH 8.0, 1.67 mM Mg^{++} 0.166 mM $NADP^+$, 20 µg enzyme protein and isocitrate and α-ketoglutarate as indicated.

6b) Replot of slopes against inhibitor concentrations.

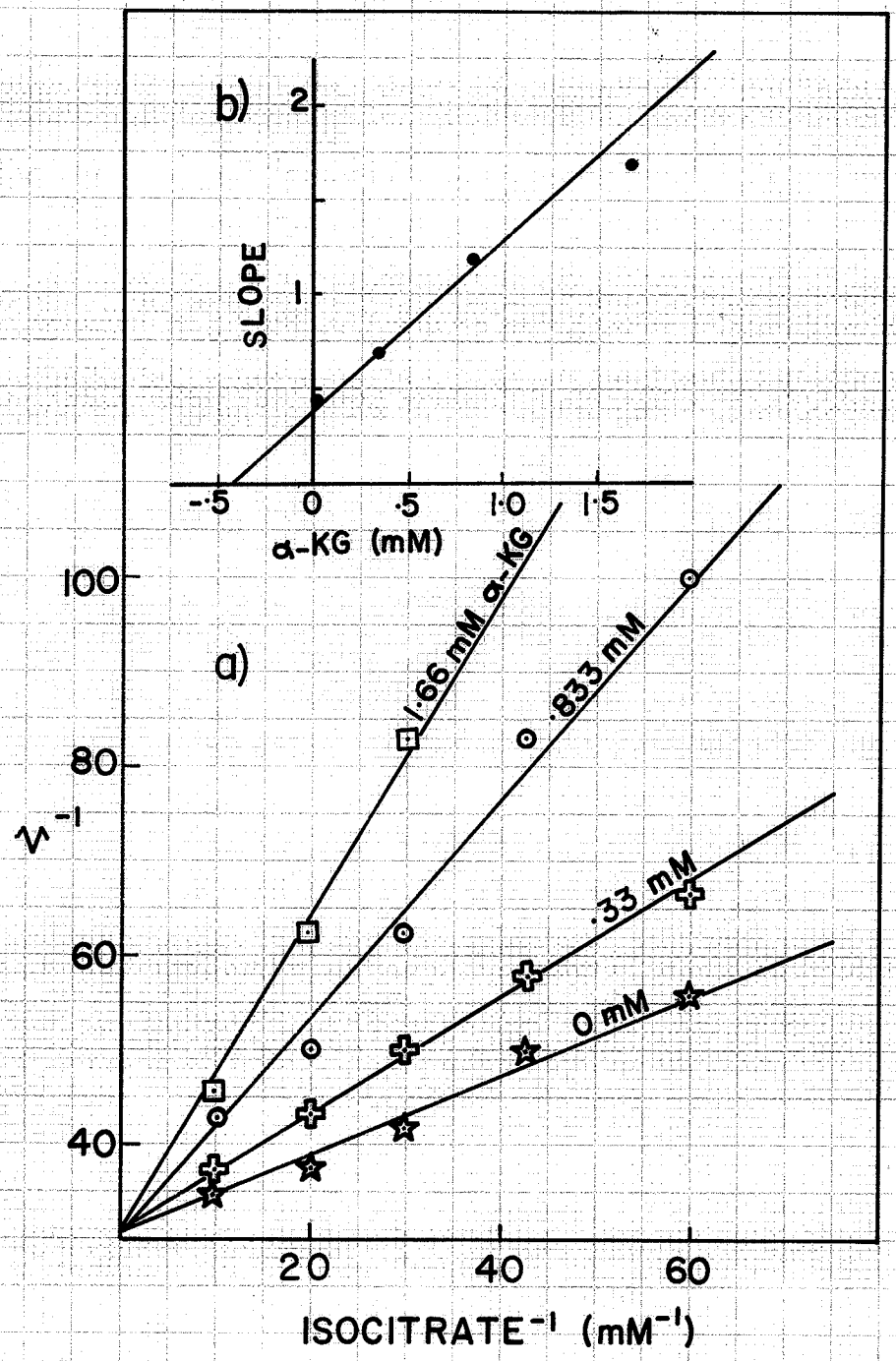

Fig. 7a) Product inhibition of α-ketoglutarate on the reduction of $NADP^+$ by B. emersonii $NADP^+$ sp. isocitrate dehydrogenase. The reaction system contained 66.67 mM tris-acetate buffer, pH 8.0, 1.67 mM Mg^{++}, 0.10 mM isocitrate, 20 μg enzyme protein and $NADP^+$ and α-ketoglutarate as indicated.

7b) Replot of intercepts against inhibitor concentrations.

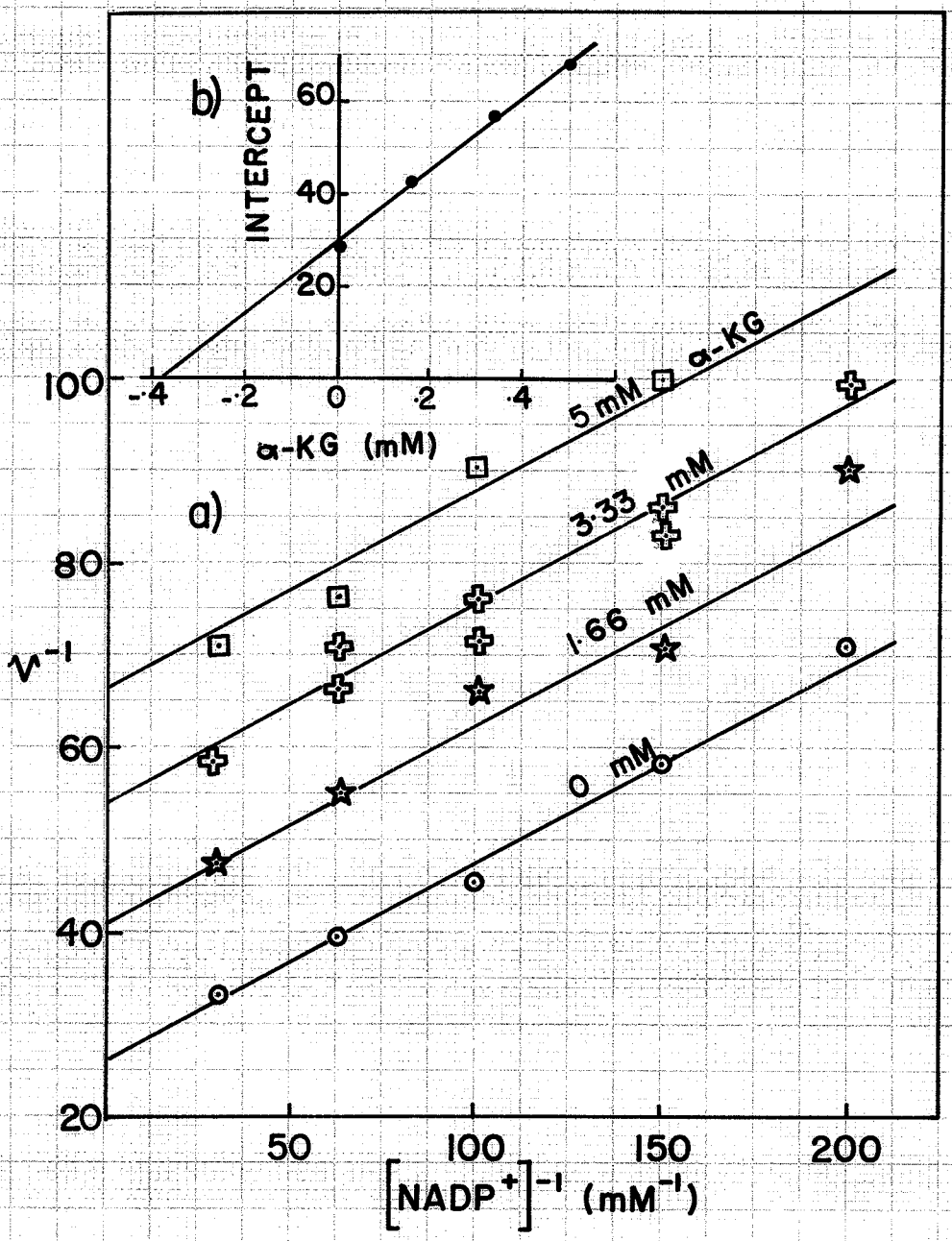
b)
INTERCEPT
60
40
20
-.4
-.2
0
.2
.4
α-KG (mM)
a)
100
80
60
40
20
v⁻¹
5 mM α-KG
3.33 mM
1.66 mM
0 mM
50
100
150
200
[NADP⁺]⁻¹ (mM⁻¹)

TABLE II

Product inhibition of $NADP^+$ specific isocitrate dehydrogenase by α-ketoglutarate

α-KG (mM)	Velocity (ΔA 340 mμ min^{-1})		
	0.10 mM isocitrate	0.33 mM isocitrate	0.66 mM isocitrate
0	0.025	0.026	0.026
1.66	0.018	0.023	0.022
3.33	0.015	0.021	0.022
5.0	0.013	0.020	0.022

The reaction mixture contained 0.0166 mM $NADP^+$, isocitrate and α-ketoglutarate as indicated, 1.66 mM Mg^{++}, 66.67 mM tris-acetate buffer, pH 8.0, and 20 μg enzyme protein.

Fig. 8a) Product inhibition of NADPH on the decarboxylation of isocitrate by B. emersonii $NADP^+$ specific isocitrate dehydrogenase. The reaction system contained 66.67 mM tris-acetate buffer, pH 8.0, 1.67 mM Mg^{++}, 0.50 mM or 0.167 mM NADP as indicated, 20 µg enzyme protein, and isocitrate and NADPH as indicated.

8b) Replot of intercepts against inhibitor concentrations.

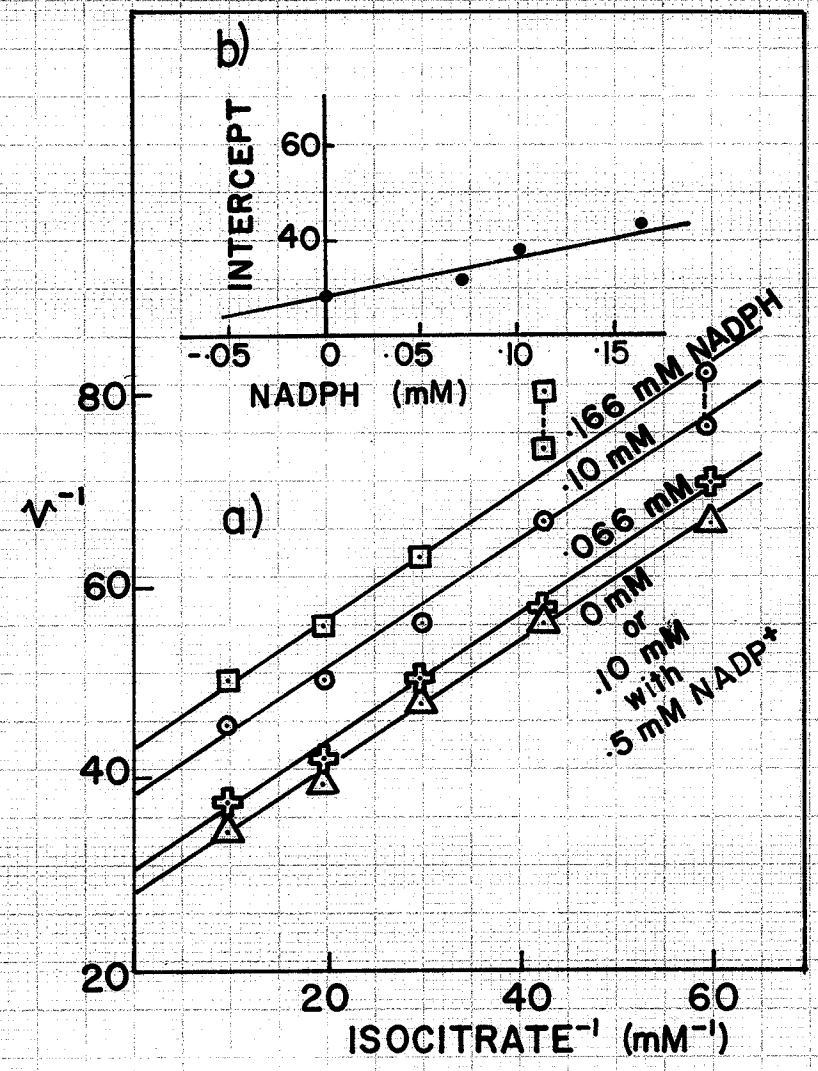
b)
INTERCEPT
60
40
-.05
0
.05
.10
.15
NADPH (mM)
.166 mM NADPH
.10 mM
.066 mM
0 mM
or
.10 mM
with
.5 mM NADP+
a)
v^{-1}
80
60
40
20
20
40
60
ISOCITRATE^{-1} (mM^{-1})

with 0.01 mM α-ketoglutarate (Fig. 8).

5. Isocitrate : Bicarbonate

Using bicarbonate as the inhibitor against isocitrate as the variable substrate results in a competitive pattern under conditions of very high inhibitor concentration (Fig. 9). The replot of slopes is linear and the K_i for bicarbonate is found to be 22 mM (Fig. 9b). The carbon dioxide content of the reaction solution was not determined, so that it is impossible to give quantitative validity to these results, except to conclude that very high relative bicarbonate concentrations are required for inhibition.

6. $NADP^+$: Bicarbonate

With $NADP^+$ as the variable substrate, bicarbonate again inhibits only at extremely high concentrations. The pattern is noncompetitive with a linear replot (Fig. 10 and 10b). The K_i under these conditions, obtained by a replot of the intercepts, is approximately 150 mM (Fig. 10c).

A summary of the preceding kinetic data is found in Table III.

The Reductive Decarboxylation of α-ketoglutarate

Initial velocity studies of the reductive decarboxylation of α-ketoglutarate were done to assess the regulatory potential of the reaction. When the substrate NADPH was varied for different fixed concentrations of α-ketoglutarate while the bicarbonate concentration was kept at 16.67 mM, a family of sigmoid curves resulted (Fig. 11). Double reciprocal plots resulted in a set of curved lines (Fig. 11b). When the substrate α-ketoglutarate was varied, a family of apparently hyperbolic

Fig. 9a) Product inhibition of HCO_3^- on the decarboxylation of isocitrate by B. emersonii NADP sp. isocitrate dehydrogenase. The reaction system contained 66.67 mM tris-acetate buffer, pH 8.5, 1.67 mM Mg^{++}, 0.166 mM $NADP^+$, 20 µg enzyme protein, and isocitrate and HCO_3^- as indicated.

9b) Replot of slopes against inhibitor concentrations.

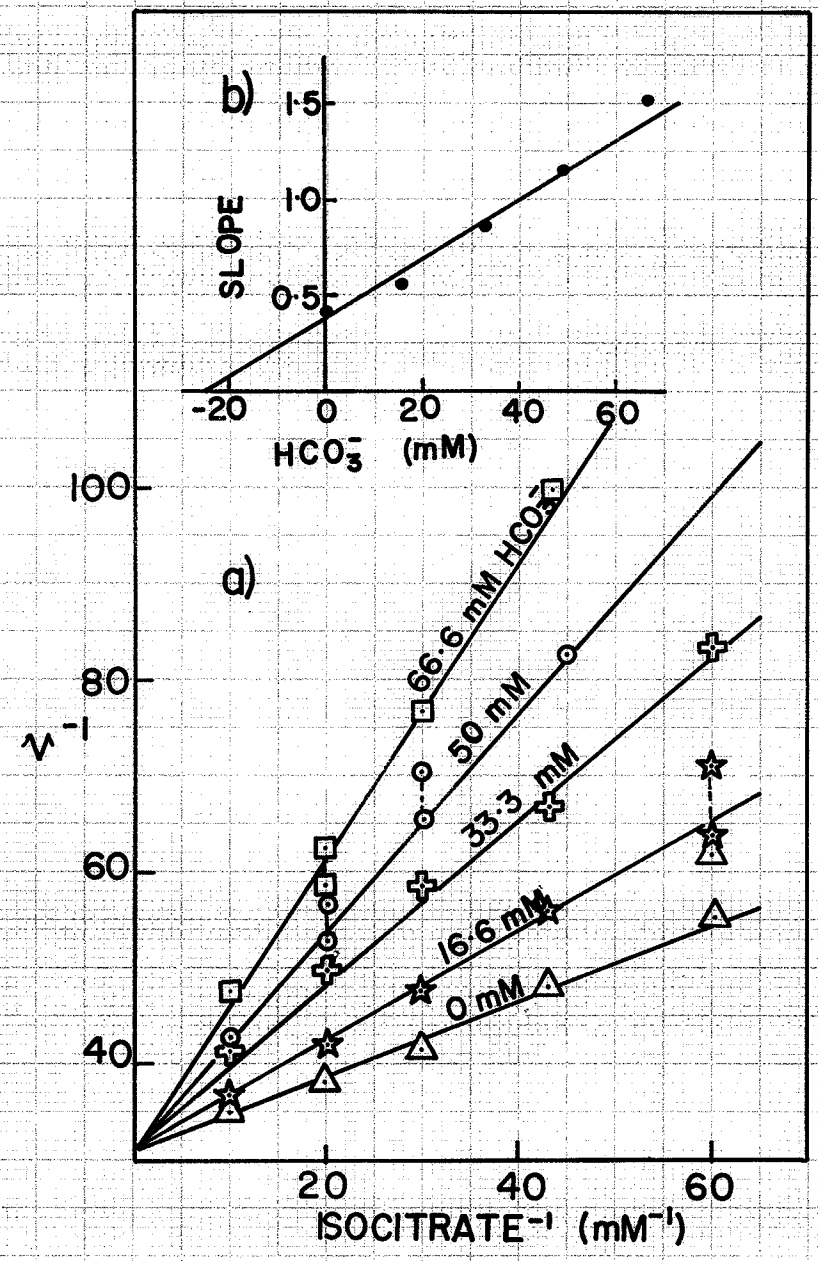
b)
SLOPE
1·5
1·0
0·5
-20
0
20
40
60
HCO3- (mM)
a)
100
80
60
40
v-1
66·6 mM HCO3-
50 mM
33·3 mM
16·6 mM
0 mM
20
40
60
ISOCITRATE-1 (mM-1)

Fig. 10a) Product inhibition of HCO_3^- on the reduction of $NADP^+$ by B. emersonii $NADP^+$ specific isocitrate dehydrogenase. The reaction system contained 66.67 mM tris-acetate buffer, pH 8.5, 1.67 mM Mg^{++}, 0.33 mM isocitrate, 20 µg enzyme protein and $NADP^+$ and HCO_3^- as indicated.

10b) Replot of intercepts against inhibitor concentration.

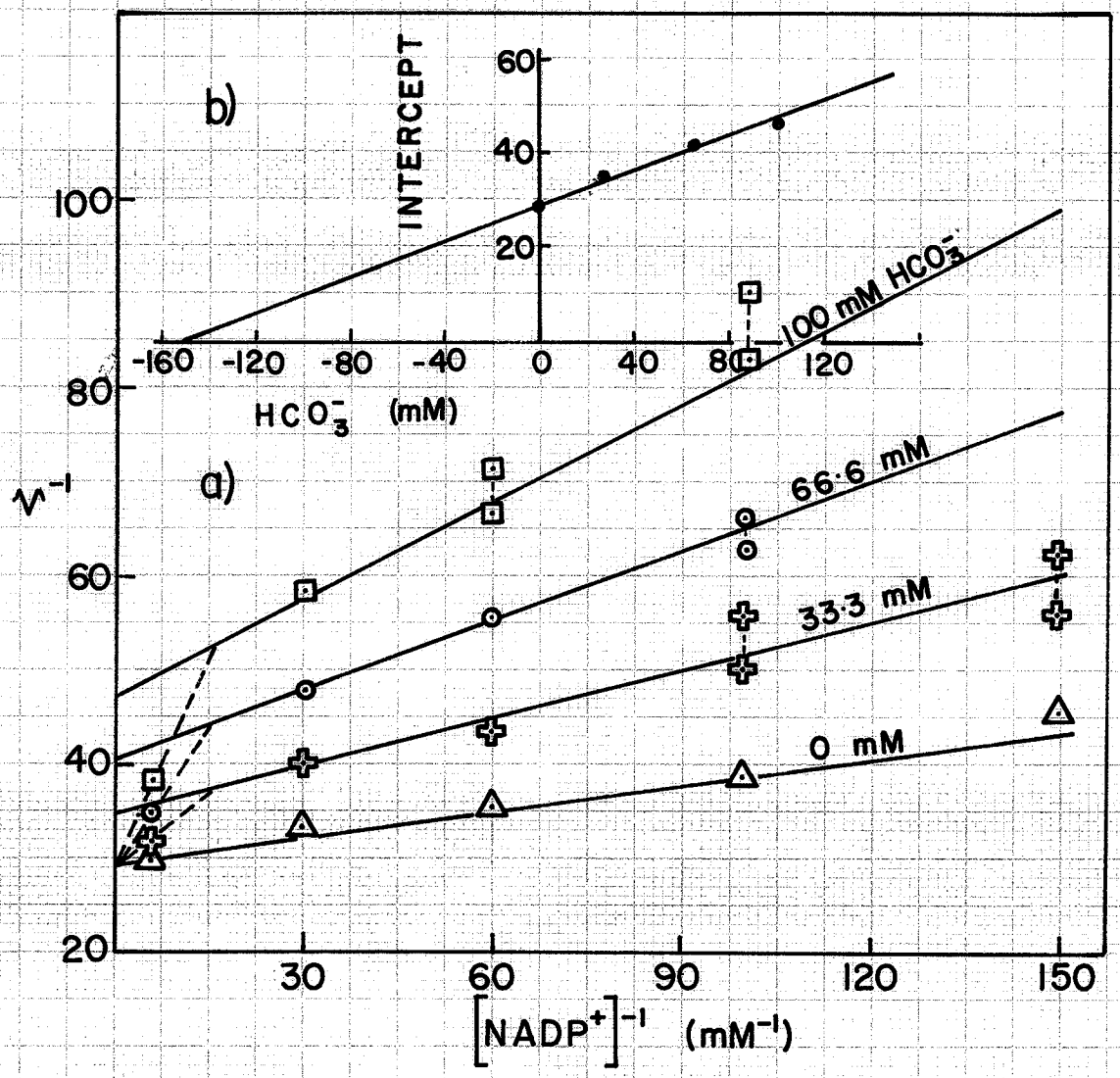
b)
INTERCEPT
60
40
20
100
80
60
40
20
-160
-120
-80
-40
0
40
80
120
HCO_3^- (mM)
100 mM HCO_3^-
a)
v^{-1}
66·6 mM
33·3 mM
0 mM
30
60
90
120
150
$[NADP^+]^{-1}$ (mM^{-1})

TABLE III

Kinetic Studies on $NADP^+$ specific Isocitrate Dehydrogenase from Blastocladiella emersonii

A. Initial Velocity Studies

Variable Substrate	Fixed Substrate	Double Reciprocal Plots	Slope Replot	Intercept Replot	Constants
Isocitrate	$NADP^+$	linear-parellel	-	linear	K_m ($NADP^+$)=6.6 μM
NADP	isocitrate	linear-parallel	-	linear	K_m (isocitrate)=15 μM

B. Product Inhibition Studies

Product Inhibitor	Varying Substrate	Double Reciprocal Plots	Slope Replot	Intercept Replot	Inhibition		Constants
					Fixed Substrate Unsaturating	Fixed Substrate Saturating	
NADPH	$NADP^+$	linear-intersecting	linear	-	-	Competitive	K_i=21 μM
α-KG	isocitrate	linear-intersecting	linear	-	-	Competitive	K_i=450 μM
α-KG	$NADP^+$	linear-parallel	-	linear	Uncompetitive	No Inhibition	-
NADPH	isocitrate	linear-parallel	-	linear	Uncompetitive	No Inhibition	-
HCO_3^-	isocitrate	linear-intersecting	linear	-	-	Competitive	K_i= 22 mM
HCO_3^-	$NADP^+$	linear-intersecting	-	linear	-	Noncompetitive	K_i= 150 mM

Fig. 11. Initial velocity studies of the reductive decarboxylation of a α-ketoglutarate by the $NADP^+$ specific isocitrate dehydrogenase from B. emersonii.

a) Rate concentration plots of velocity against NADPH concentration. The reaction mixture contained 66.67 mM tris-acetate buffer, pH 7.2, 16.67 mM HCO_3^-, 1.66 mM Mg^{++}, NADPH and α-ketoglutarate as indicated, and 20 µg enzyme protein.

b) Double reciprocal plots of data reported in Fig. 11a.

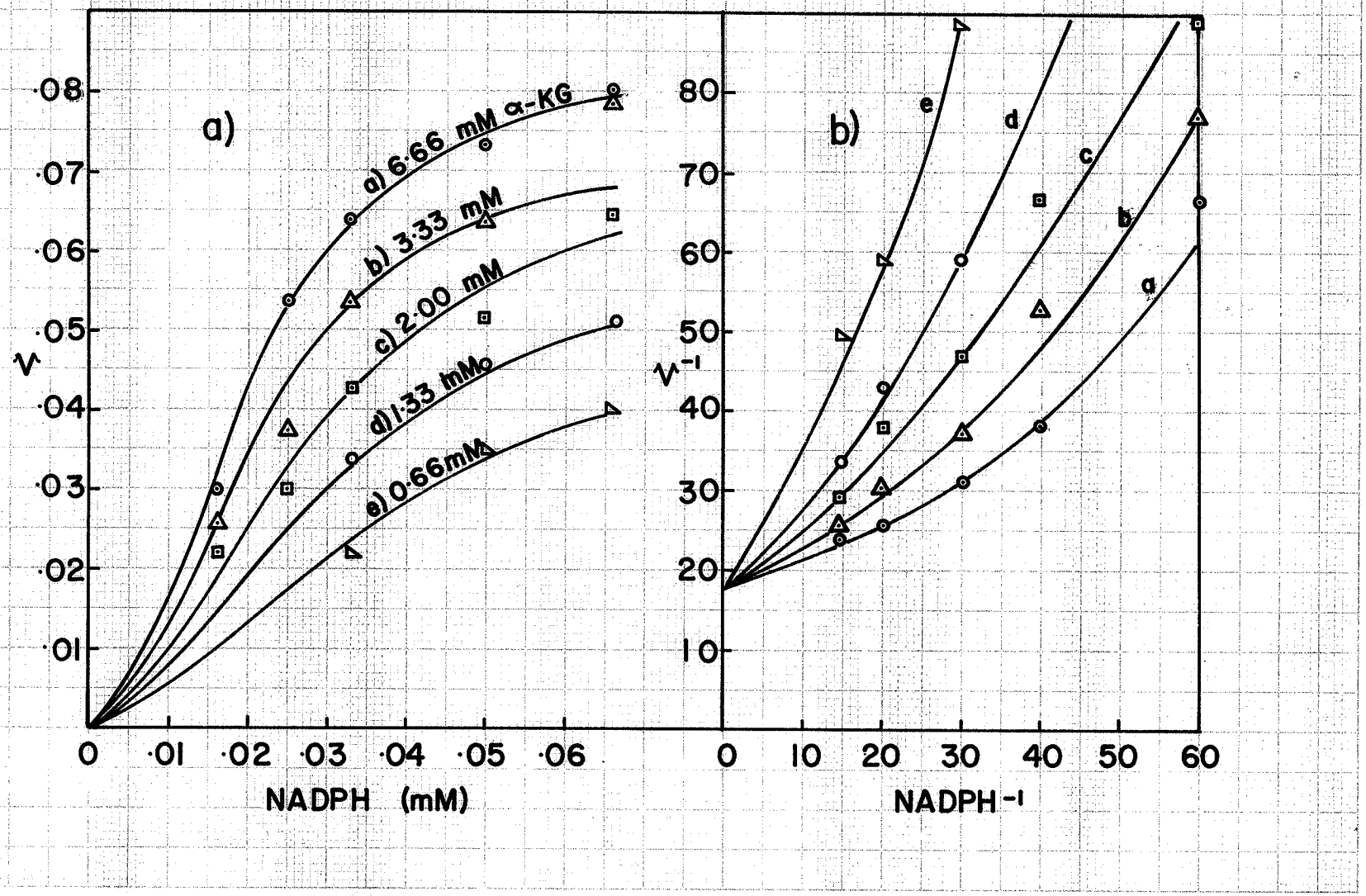
a)
b)
a) 6·66 mM α-KG
b) 3·33 mM
c) 2·00 mM
d) 1·33 mM
e) 0·66mM
v
v⁻¹
NADPH (mM)
NADPH⁻¹
·08
·07
·06
·05
·04
·03
·02
·01
0
·01
·02
·03
·04
·05
·06
80
70
60
50
40
30
20
10
0
10
20
30
40
50
60

lines resulted (Fig. 12). The double reciprocal replots, however, did not appear linear (Fig. 12b). The experiment was repeated using Mn^{++} (Fig. 13). In this case the curves are sigmoid, and the double reciprocal plots curved positively as was observed when NADPH was used as the variable substrate (Fig. 13b).

The Effect of Citrate

The effect of citrate on the oxidative decarboxylation of isocitrate is seen in Fig. 14. Several concentrations of citrate are held constant while isocitrate is varied. At saturating isocitrate, citrate up to 10 mM has very little effect, but as isocitrate decreases, inhibition by citrate increases, approaching total inhibition at 0.033 mM isocitrate and 10 mM citrate. The curves appear sigmoid with increasing sigmoidicity as isocitrate decreases.

The effect of citrate on the reductive carboxylation of α-ketoglutarate is seen in Fig. 15. Again, citrate is an inhibitor against a varying α-ketoglutarate concentration. As α-ketoglutarate decreases, the effect of citrate increases, but the inhibition pattern does not change. Citrate inhibition appears to approach a maximum at 6 mM.

The Effect of Nucleotides

Due to the known importance of nucleotide effectors for the NAD^+ specific IDH from B. emersonii, experiments were done to elucidate their effect on the $NADP^+$ specific IDH. AMP, ADP, and ATP at 3.33 mM were used with saturating concentrations of isocitrate and unsaturating concentrations of $NADP^+$ (Table IV). Inhibition of the oxidative

Fig. 12. Initial velocity studies of the reductive decarboxylation of α-ketoglutarate by the $NADP^+$ specific isocitrate dehydrogenase from *B. emersonii*.

a) Rate concentration plots of velocity against α-ketoglutarate concentration. The reaction mixture contained 66.67 mM tris-acetate buffer, pH 7.2, 16.67 mM HCO_3^- 1.66 mM Mg^{++}, NADPH and α-ketoglutarate as indicated, and 50 µg enzyme protein.

b) Double reciprocal plots of data reported in Fig. 12a.

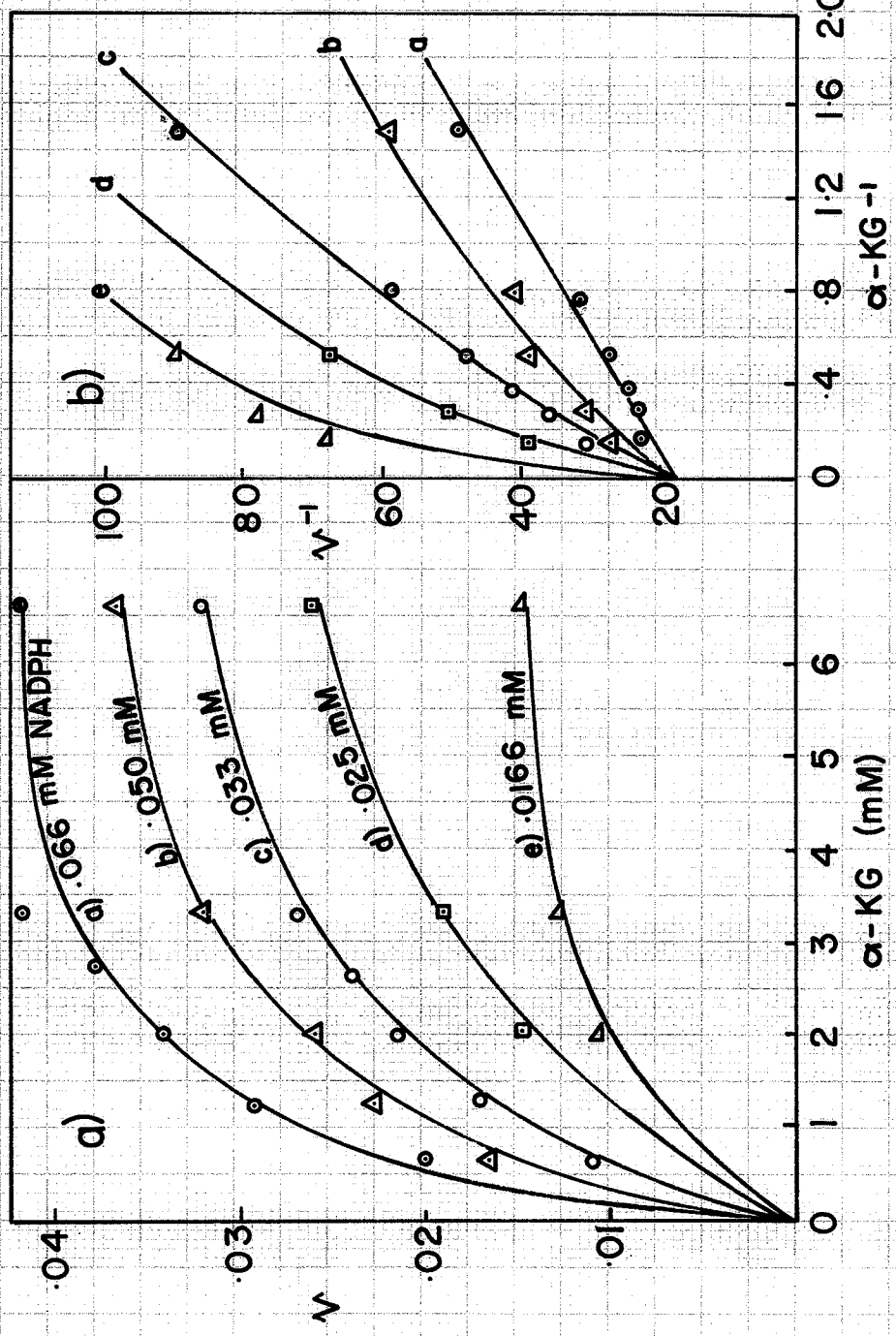
a)
b)
a) .066 mM NADPH
b) .050 mM
c) .033 mM
d) .025 mM
e) .0166 mM
v
v⁻¹
α-KG (mM)
α-KG⁻¹
.04
.03
.02
.01
0
1
2
3
4
5
6
20
40
60
80
100
.4
.8
1.2
1.6
2.0

Fig. 13. Initial velocity studies of the reductive decarboxylation of α-ketoglutarate by the NADP specific isocitrate dehydrogenase from B. emersonii.

a) Rate concentration plots of velocity against α-ketoglutarate concentration. The reaction system contained 66.67 mM tris-acetate buffer, pH 7.2, 100 mM HCO_3^-, NADPH and α-ketoglutarate as indicated, 1.66 mM Mn^{++}, and 50 µg enzyme protein.

b) Double reciprocal plots of the data reported in Fig. 13a.

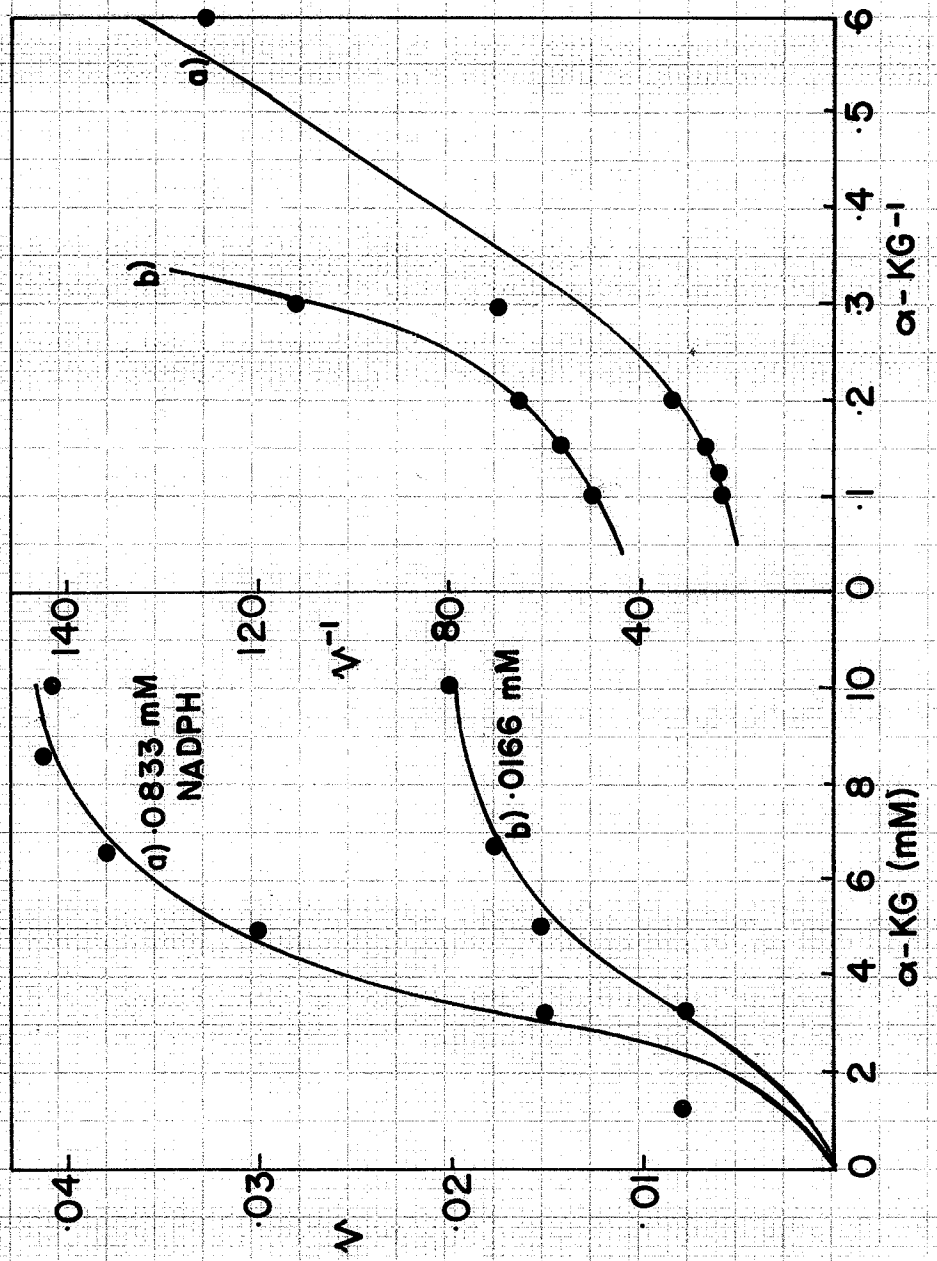

Fig. 14. The inhibition of the oxidative decarboxylation of isocitrate by $NADP^+$ specific isocitrate dehydrogenase from B. emersonii by citrate. The reaction system contained 0.33 mM $NADP^+$, 66.67 mM tris-acetate buffer, pH 8.0, 1.66 mM Mn^{++}, isocitrate and citrate as indicated, and 20 µg enzyme protein.

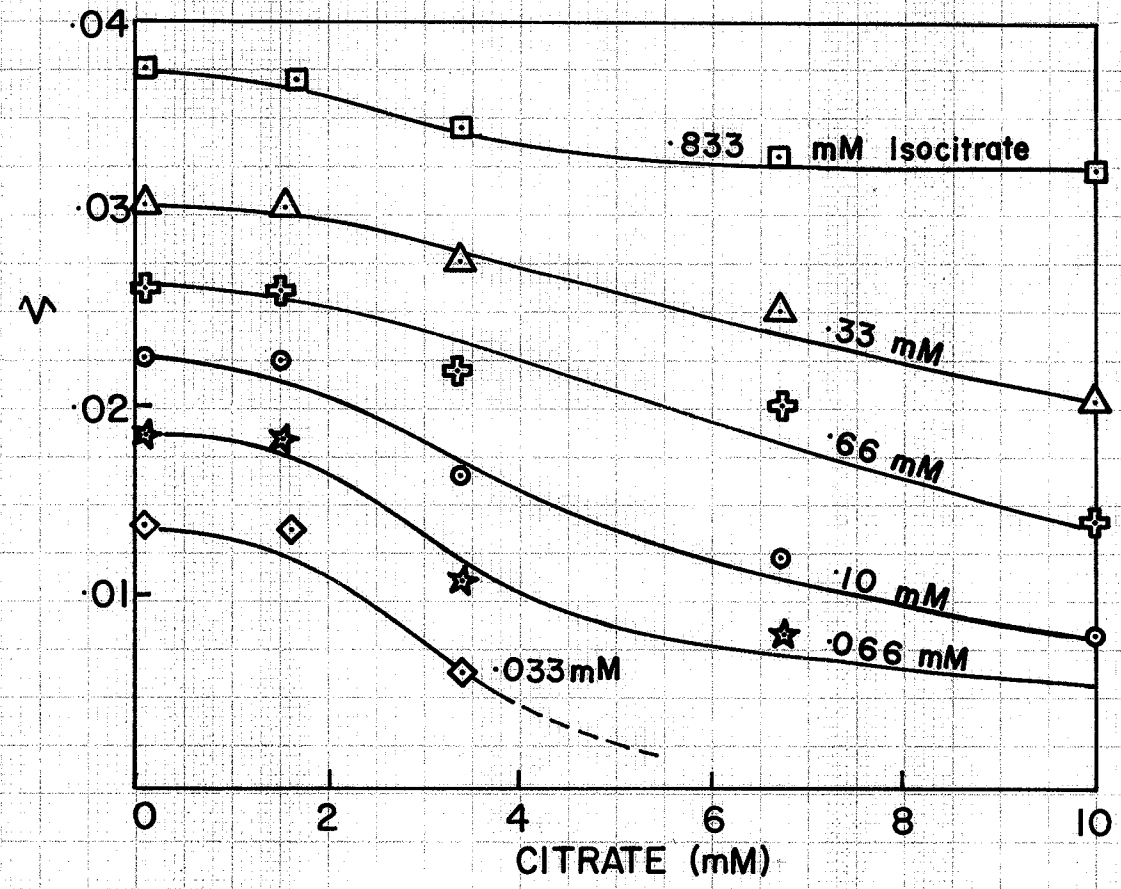
·04
·03
·02
·01
v
·833 mM Isocitrate
·33 mM
·66 mM
·10 mM
·066 mM
·033mM
0
2
4
6
8
10
CITRATE (mM)

Fig. 15. The inhibition of the reductive carboxylation of α-ketoglutarate by $NADP^+$ specific isocitrate dehydrogenase from B. emersonii by citrate. The reaction system contained 66.67 mM tris-acetate buffer, pH 7.2, 0.066 mM NADPH, 1.66 mM Mg^{++}, 16.67 mM HCO_3^-, α-ketoglutarate and citrate as indicated, and 50 µg enzyme protein.

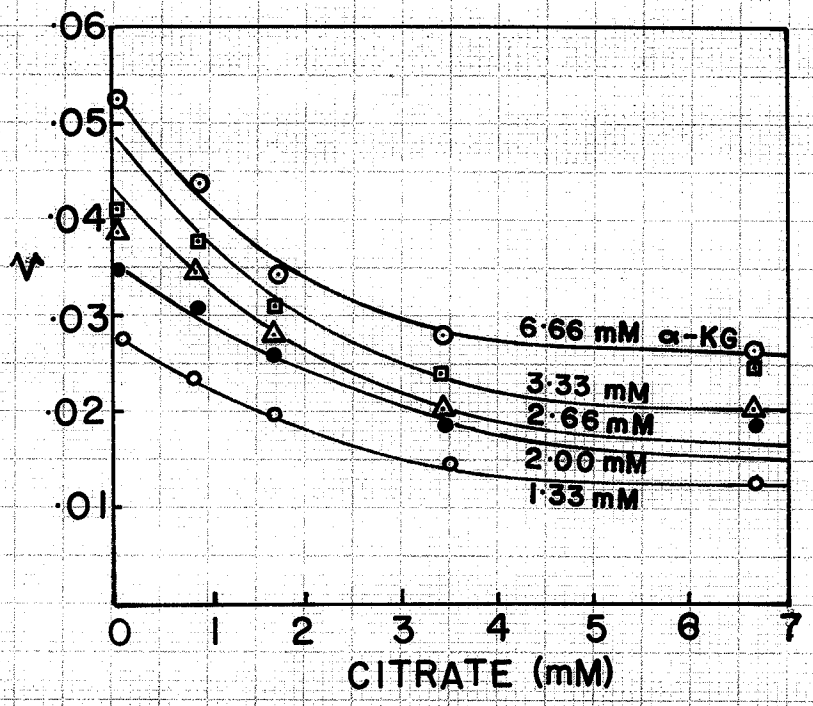
·06
·05
·04
·03
·02
·01
V
6·66 mM α-KG
3·33 mM
2·66 mM
2·00 mM
1·33 mM
0
1
2
3
4
5
6
7
CITRATE (mM)

TABLE IV

The effect of nucleotides on the oxidative decarboxylation of isocitrate by $NADP^+$ specific isocitrate dehydrogenase from B. emersonii.

Nucleotide	v/v_o
AMP	0.80
ADP	0.28
ATP	0.22

The reaction system contained 0.33 mM isocitrate, 0.033 mM $NADP^+$, 66.67 mM tris-acetate buffer, pH 8.0, 1.66 mM Mg^{++}, 3.33 mM nucleotide as indicated, and 20 µg enzyme protein. v_o= enzyme velocity with no inhibitor, v = enzyme velocity in the presence of inhibitor.

TABLE V

The effect of nucleotides on the reductive carboxylation of α-ketoglutarate by $NADP^+$ specific isocitrate dehydrogenase from B. emersonii.

Nucleotide	v/v_o
AMP	0.55
ADP	0.61
ATP	0.50

The reaction system contained 1.66 mM α-ketoglutarate 0.033 mM NADPH, 16.67 mM HCO_3^-, 66.67 mM tris-acetate buffer, pH 7.2, 1.66 mM Mg^{++}, 3.33 mM nucleotide as indicated, and 50 µg of enzyme protein. v_o = enzyme velocity with no inhibitor, v = enzyme velocity in the presence of inhibitor.

decarboxylation of isocitrate was observed, but the pattern was not differential, ADP and ATP inhibiting equally.

The effect of the same nucleotides on the reductive decarboxylation of α-ketoglutarate may be seen in Table V. Again inhibition is observed, but again there is no differential effect, with all three nucleotides inhibiting equally.

The Effect of Ionic Strength

Table VI records the effect on enzyme velocity when the ionic strength of the reaction system is varied. It can be seen that the enzyme is insensitive to changes in ionic strength over the range employed.

Ionic strength is expressed as $\Gamma/2$, which is defined by the formula:

$$\Gamma/2 = 1/2 \sum_i C_i Z_i^2 ,$$

in which C_i is the molar concentration of the "i"th ion and Z_i is the charge on the "i"th ion. In this experiment two ions were present in sufficient concentration to affect the ionic strength of the reaction system significantly, namely, tris and acetate. Consequently $\Gamma/2$ values were calculated in the following manner:

$$\Gamma/2 = 1/2 \left([\text{tris}] \cdot 1^2 + [\text{acetate}] \cdot 1^2 \right)$$

II. NAD^+ specific Isocitrate Dehydrogenase

This report is an extension of the study of initial velocity patterns of the NAD^+ specific IDH from B. emersonii* (LeJohn et al, 1969a). In

*NAD^+ specific enzyme, purified 400 fold, was supplied by Dr. H.B. LeJohn. The purification procedure may be found in the report of LeJohn et al, 1969a.

TABLE VI

The effect of ionic strength on the activity of NADP specific isocitrate dehydrogenase from B. emersonii.

$\Gamma/2$	v/v_o
0.01	1.00
0.02	0.99
0.04	0.98
0.08	1.00

The reaction mixture contained 0.33 mM isocitrate, 0.166 mM $NADP^+$, 1.66 mM Mg^{++}, 66.67 mM tris-acetate buffer, pH 8.0 and 20 µg enzyme protein.

particular it investigates the effect of varying ionic strength on the enzyme.

Initial Velocity Studies in the Absence of Activators

When isocitrate was varied for several fixed concentrations of NAD^+ (Fig. 16), double reciprocal plots of the data result in a family of curved lines. A Hill replot (see section II of the "Discussion") of the data yields a set of lines with slopes approximately equal to 2 (Fig. 16b). The slope increases with an increase in NAD^+ concentration.

When NAD^+ was the variable substrate and isocitrate was held at fixed concentrations, the double reciprocal plots were again non-linear, but the curved lines were inflected in the region of 0.3 mM NAD^+ (Fig. 17). Hill replots of the data were complex (Fig. 16b). At high NAD^+ concentrations, entirely different, higher, slopes were obtained for two of the lines than at low NAD^+ concentrations. When considering only the slopes at high NAD^+ concentrations it could be said that these slopes decrease as isocitrate concentration increases.

The Effect of Ionic Strength

Figure 18 shows that increasing ionic strength inhibits enzyme activity in the absence of the activator AMP. The nature of this inhibition was elaborated by repeating the initial velocity studies at various ionic concentrations. When isocitrate was varied against different fixed ionic concentrations, the data recorded in Fig. 19 was obtained. Hill replots of the data (Fig. 19b), reveal that as ionic strength increases, the slope of the line increases. When NAD^+ was the variable substrate, the double reciprocal plots were inflected

Fig. 16. Initial velocity studies of the oxidative decarboxylation of isocitrate by NAD^+ specific isocitrate dehydrogenase from B. emersonii.

a) Double reciprocal plots of rate against isocitrate concentration. The reaction system contained 66.67 mM tris-acetate buffer, pH 7.5, 1.66 mM Mn^{++}, 5 µg enzyme protein, and isocitrate and NAD^+ as indicated.

b) Hill replot of the data reported in Fig. 16a.

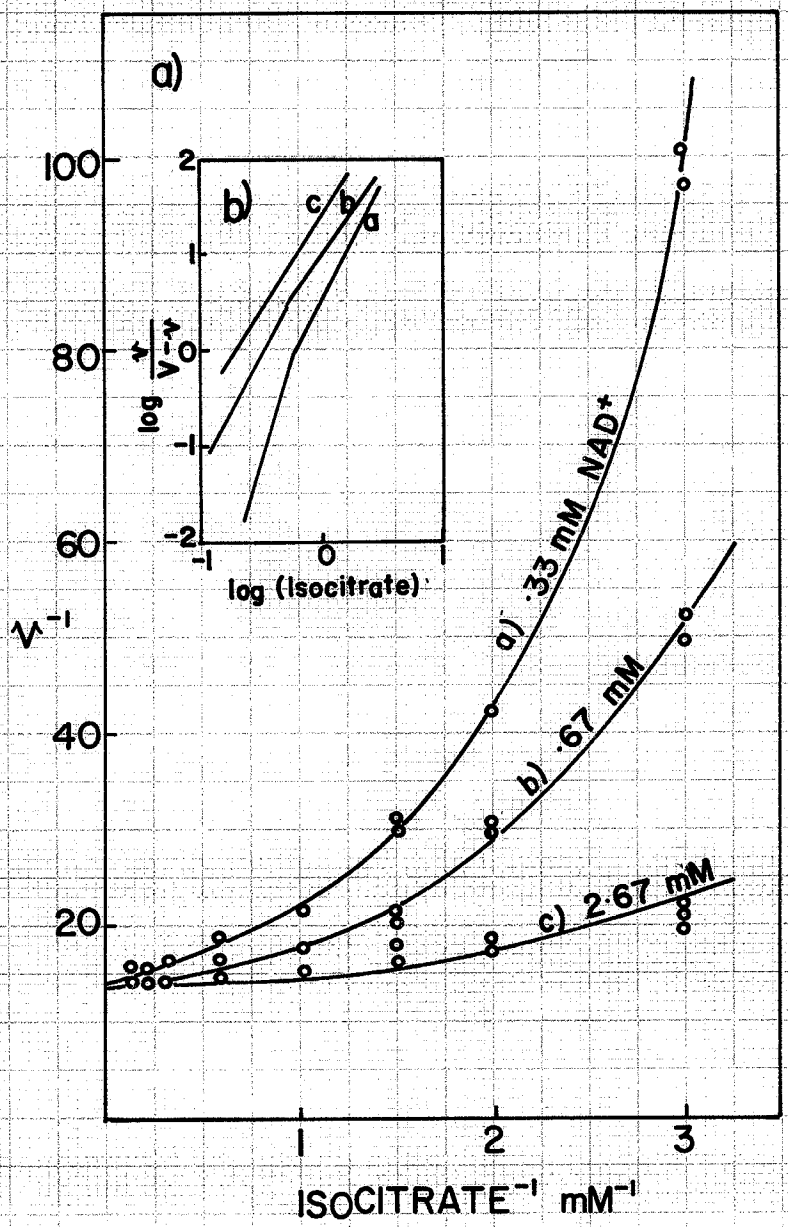
a)
b)
c
b
a
log $\frac{v}{V-v}$
log (Isocitrate)
v^{-1}
a) .33 mM NAD+
b) .67 mM
c) 2.67 mM
ISOCITRATE^{-1} mM^{-1}

Fig. 17. Initial velocity studies of the oxidative decarboxylation of isocitrate by NAD^+ specific isocitrate dehydrogenase from B. emersonii.

a) Double reciprocal plots of rate against NAD^+ concentration. The reaction system contained 66.67 mM tris-acetate buffer, pH 7.5, 1.66 mM Mn^{++}, 5 µg enzyme protein, and isocitrate and NAD^+ as indicated.

b) Hill replot of the data reported in Fig. 17a.

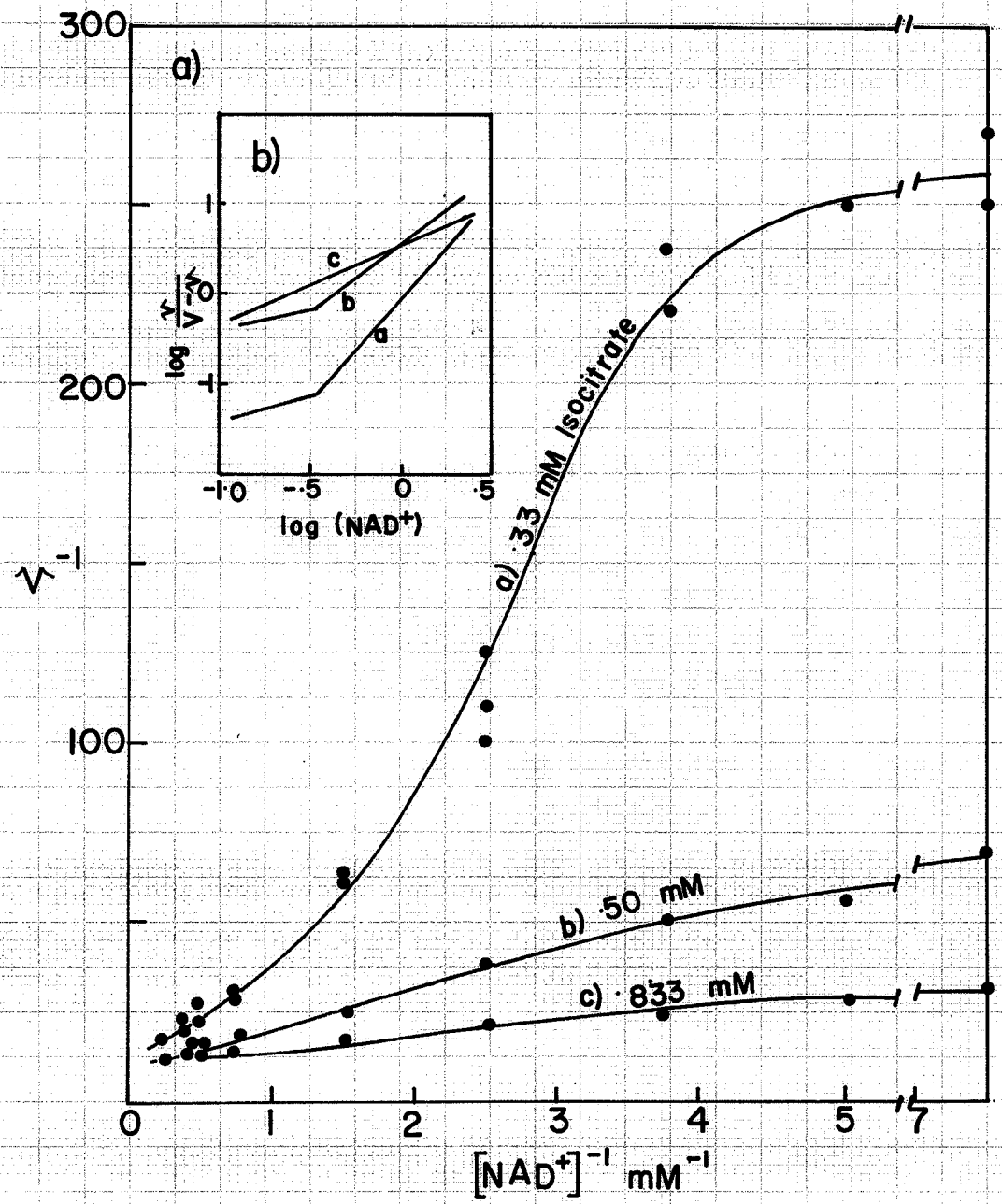
300
200
100
a)
b)
c
b
a
log $\frac{v}{V-v}$
1
0
-1
-1·0
-·5
0
·5
log (NAD+)
v^{-1}
a) ·33 mM Isocitrate
b) ·50 mM
c) ·833 mM
0
1
2
3
4
5
7
$[NAD^+]^{-1}$ mM^{-1}

Fig. 18. The effect of increasing ionic strength on the activity of NAD^+ specific isocitrate dehydrogenase from B. emersonii, in the presence and absence of AMP.

The reaction system contained 33.3 mM tris-acetate buffer, pH 7.5, 3.33 mM isocitrate, 1.33 mM NAD^+, and 5 µg enzyme protein. Ionic strength was increased by the addition of NaCl or NH_4Cl. 1 mM AMP was used to counteract the ionic influence.

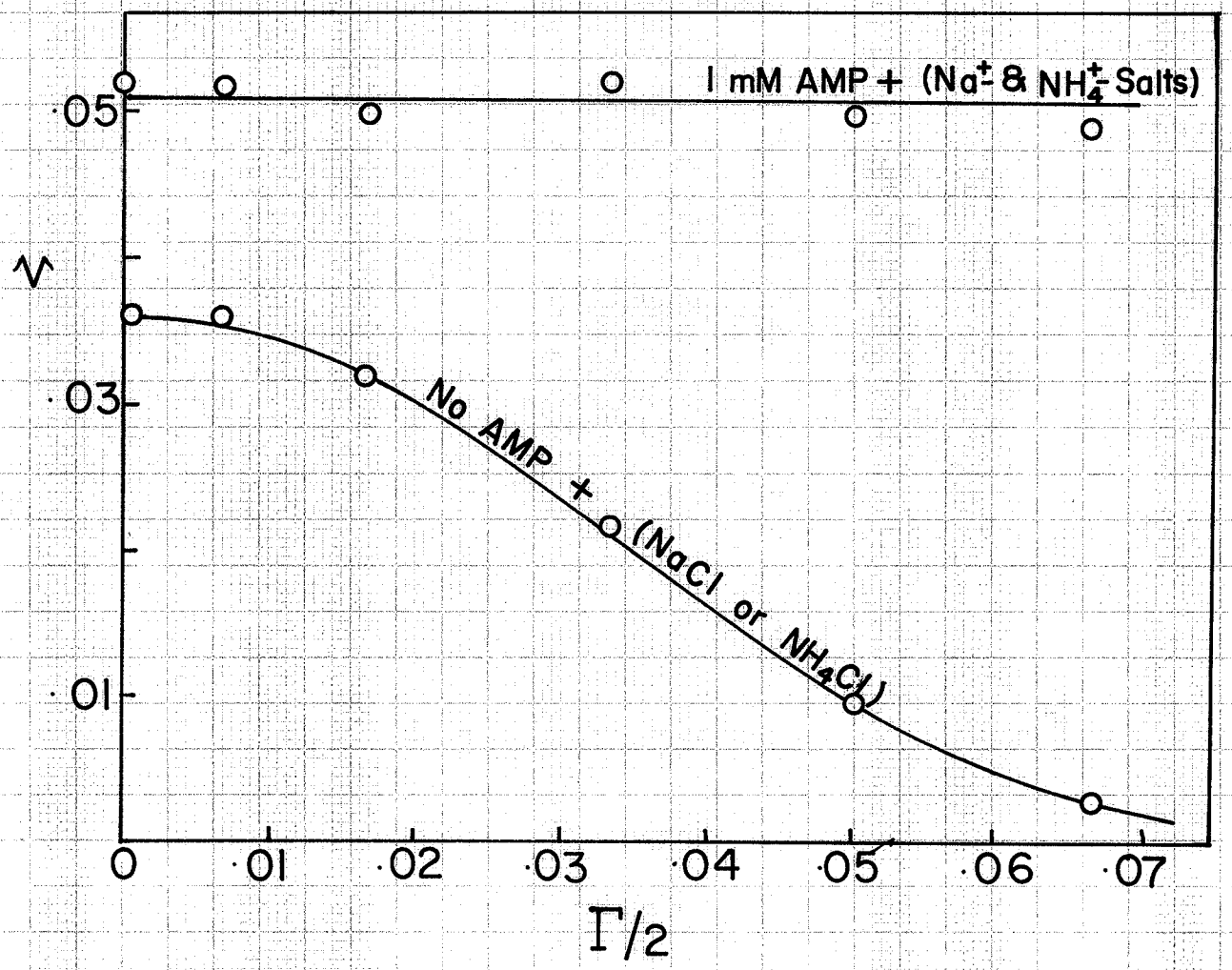
1 mM AMP + (Na+ & NH4+ Salts)
No AMP + (NaCl or NH4Cl)
ν
·05
·03
·01
0
·01
·02
·03
·04
·05
·06
·07
Γ/2

Fig. 19. The effect of varying ionic strength on the initial velocity pattern of NAD^+ specific isocitrate dehydrogenase from B. emersonii when isocitrate is the variable substrate.

a) Double reciprocal plots of rate against isocitrate concentrations in the presence of several fixed ionic concentrations. The reaction system contained tris-acetate buffer, pH 7.5, at the ionic strength indicated, 0.667 mM NAD^+, 1.66 mM Mn^{++}, isocitrate as indicated, and 4 µg of enzyme protein.

b) Hill replot of the data reported in Fig. 19a.

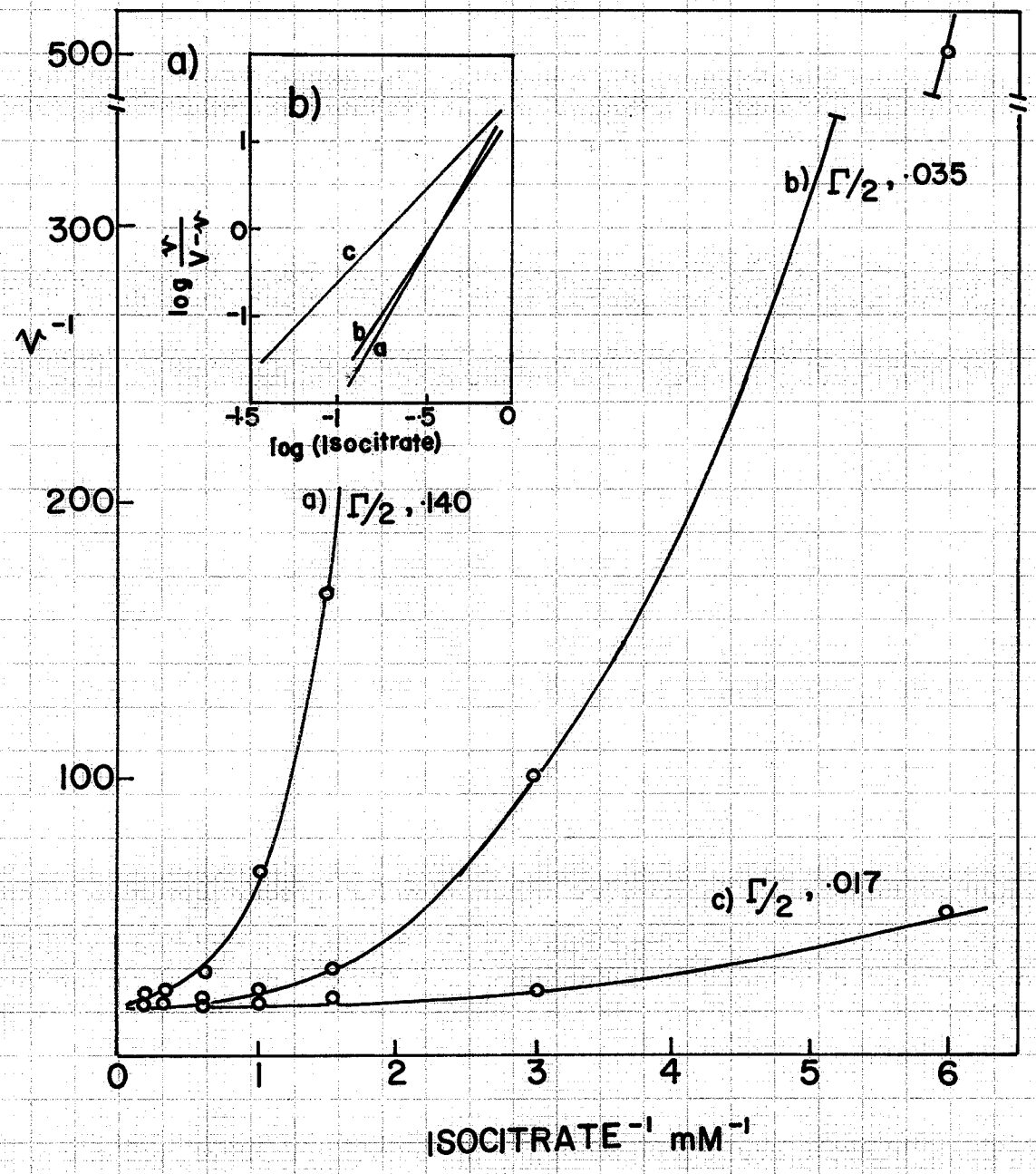
a)
b)
500
300
200
100
ν^{-1}
0
1
2
3
4
5
6
ISOCITRATE^{-1} mM^{-1}
a) Γ/2, ·140
b) Γ/2, ·035
c) Γ/2, ·017
log $\frac{v}{V-v}$
c
b
a
-1.5
-1
-.5
0
log (Isocitrate)

(Fig. 20), and the Hill replots again show a change in slope which is a function of NAD^+ concentration (Fig. 20b). At high NAD^+ concentrations, three of the lines showed a much higher slope than at low NAD^+ concentrations. When only high NAD^+ concentrations are considered it can be seen that the slope increases with an increase in ionic strength.

It has been noted (Fig. 18), that 1 mM AMP will counteract the inhibitory effect of ionic strength. At sufficiently low concentrations of AMP and citrate, however, an interaction between the effectors and ionic strength was detected. Double reciprocal plots obtained when both effectors were varied against several fixed concentrations of ions were non-linear for both effectors, but the pattern was quite different (Fig. 21). The lines for AMP were positively curved, but those for citrate were inflected. For AMP, Hill replots yielded a set of lines of slightly changing slope, but for citrate the lines had two slopes (Fig. 21b). At low citrate, the slope of the lines is much lower than at high citrate. As ionic strength increases, the slopes of the AMP lines increase and, when considering only the slopes of the citrate lines at high citrate concentration, the same trend is observed.

Fig. 20. The effect of varying ionic strength on the initial velocity pattern of NAD^+ specific isocitrate dehydrogenase from B. emersonii when NAD^+ is the variable substrate.

a) Double reciprocal plots of rate against NAD^+ concentrations in the presence of several fixed ionic concentrations. The reaction system contained tris-acetate buffer, pH 7.5, at the ionic strength indicated, 0.33 mM isocitrate, 1.66 mM Mn^{++}, NAD^+ as indicated, and 4 µg of enzyme protein.

b) Hill replot of the data reported in Fig. 20a.

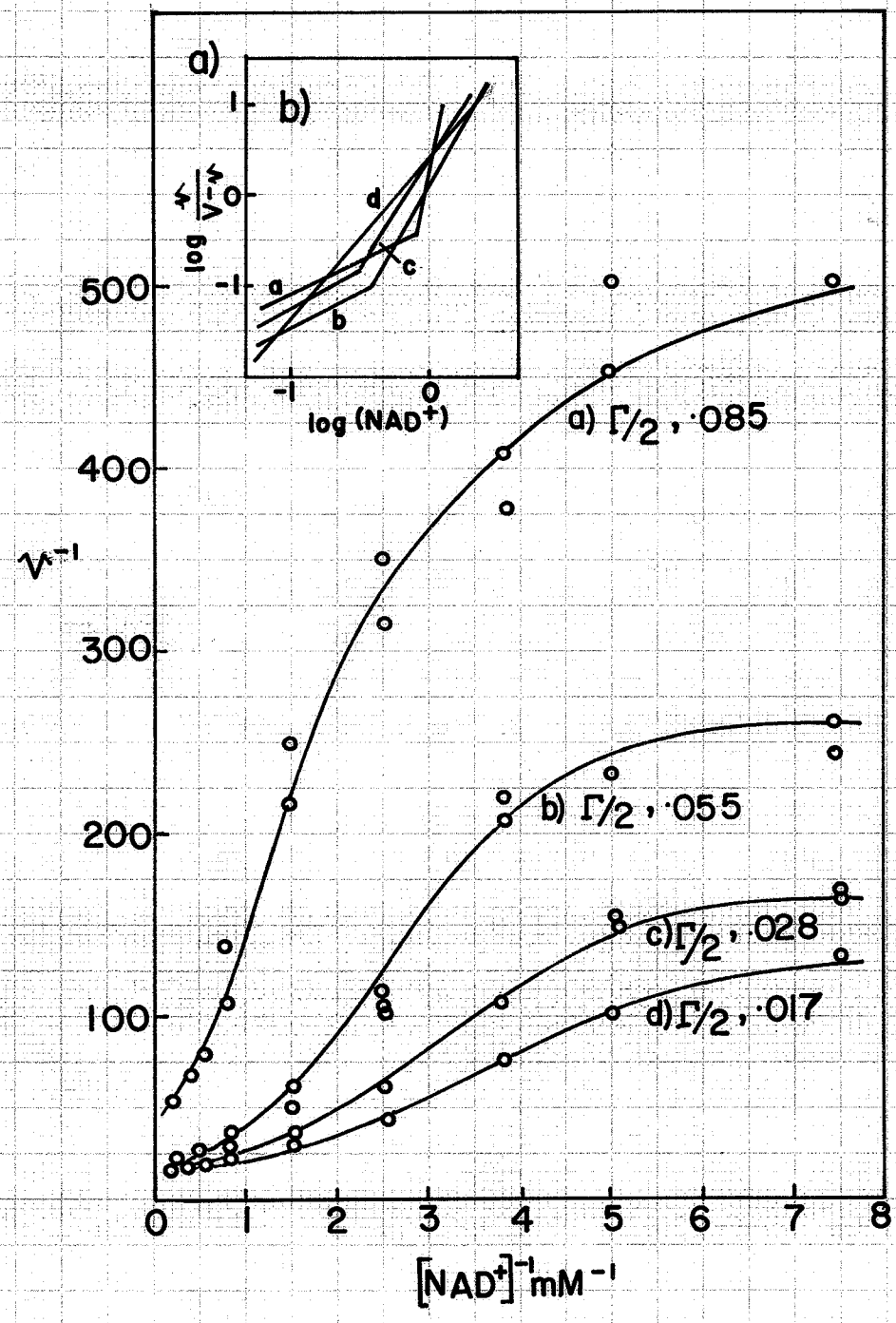
a)
b)
1
0
-1
log v/v0
a
b
c
d
-1
0
log (NAD+)
500
400
300
200
100
v-1
a) Γ/2, ·085
b) Γ/2, ·055
c) Γ/2, ·028
d) Γ/2, ·017
0
1
2
3
4
5
6
7
8
[NAD+]-1 mM-1

Fig. 21. Interactions between ionic strength and the activation of NAD^+ specific isocitrate dehydrogenase from B. emersonii by AMP and citrate.

a) Double reciprocal plots of the rate against varying activator concentrations.
The reaction system contained 1.33 mM NAD^+, 3.33 mM isocitrate, 3.33 mM Mg^{++}, 33.33 mM tris-acetate buffer, pH 7.5, and 5 µg enzyme protein. Ionic strength was increased as indicated by the addition of NaCl.

b) Hill replots of the data reported in Fig. 21b.

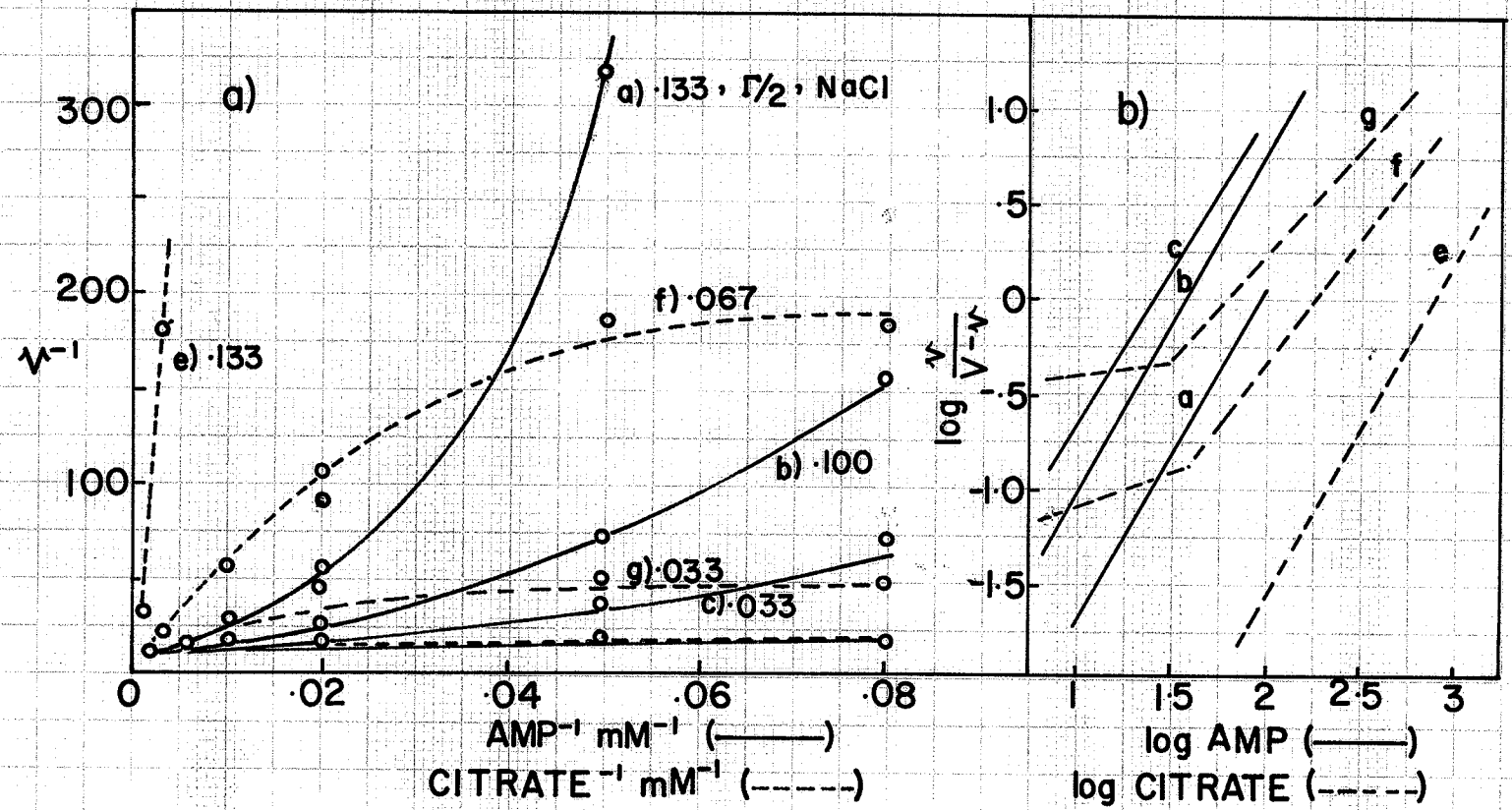
a)
300
200
100
v^{-1}
a) ·133 , Γ/2 , NaCl
f) ·067
e) ·133
b) ·100
g) ·033
c) ·033
0
·02
·04
·06
·08
AMP^{-1} mM^{-1} (———)
CITRATE^{-1} mM^{-1} (- - - - -)
b)
1·0
·5
0
-·5
-1·0
-1·5
log $\frac{v}{V-v}$
g
f
e
c
b
a
1
1·5
2
2·5
3
log AMP (———)
log CITRATE (- - - - -)

III. Glutamine Synthetase

Studies on glutamine synthetase from B. emersonii were undertaken for the following reasons: 1) Preliminary kinetic studies were done in order that the general pattern of controls on the enzyme could be elucidated; 2) The feedback inhibition pattern, discovered for this enzyme in other organisms, (Woolfolk and Stadtman, 1964), was checked for the sake of general comparison, and in order to correlate it with the regulation of the isocitrate and glutamate dehydrogenases of B. emersonii.

Purification

Purification data appears in Table VII. A 6 fold purification was achieved.

Kinetic Constants

Figures 22-24 record the effects on the rate of the reaction when each one of the three substrates is varied in turn. Double reciprocal plots appear in each figure as insets. The kinetics appear to follow classical Michaelian patterns, with the relationships between substrate concentration and enzyme velocity being hyperbolic and the double reciprocal plots linear. Approximate Michaelis constants were obtained from the double reciprocal plots, and appear in Table VIII.

Cofactor Requirement

Fig. 25 records the effect of Mn^{++} on the rate of the reaction. It is noted that the optimal range is 2 mM to 10 mM. Above 10 mM Mn^{++} begins to inhibit the reaction so that at 100 mM Mn^{++}, the initial

TABLE VII

The Purification of Glutamine Synthetase from B. emersonii

Fraction	Total Protein (mg)	Total Activity (units)	Specific Activity (units/mg)	Purification (fold)	Recovery (percent)
Crude	653	42,000	64	-	100
Step I	540	48,400	90	1.4	115
Step II	251	48,300	192	3.3	115
Step III	140	50,700	363	6	120

Fig. 22. Initial velocity studies on glutamine synthetase from B. emersonii.

a) Rate concentration plot of enzyme rate against glutamate concentration. The reaction system contained 10 mM ATP, 40 mM NH_2OH, 40 mM $MnCl_2$, 20 mM Imidazole buffer, pH 7.1, 2 mM Cleland's reagent, glutamate as indicated, and 100µl of enzyme preparation.

b) Double reciprocal plot of data reported in Fig. 22a.

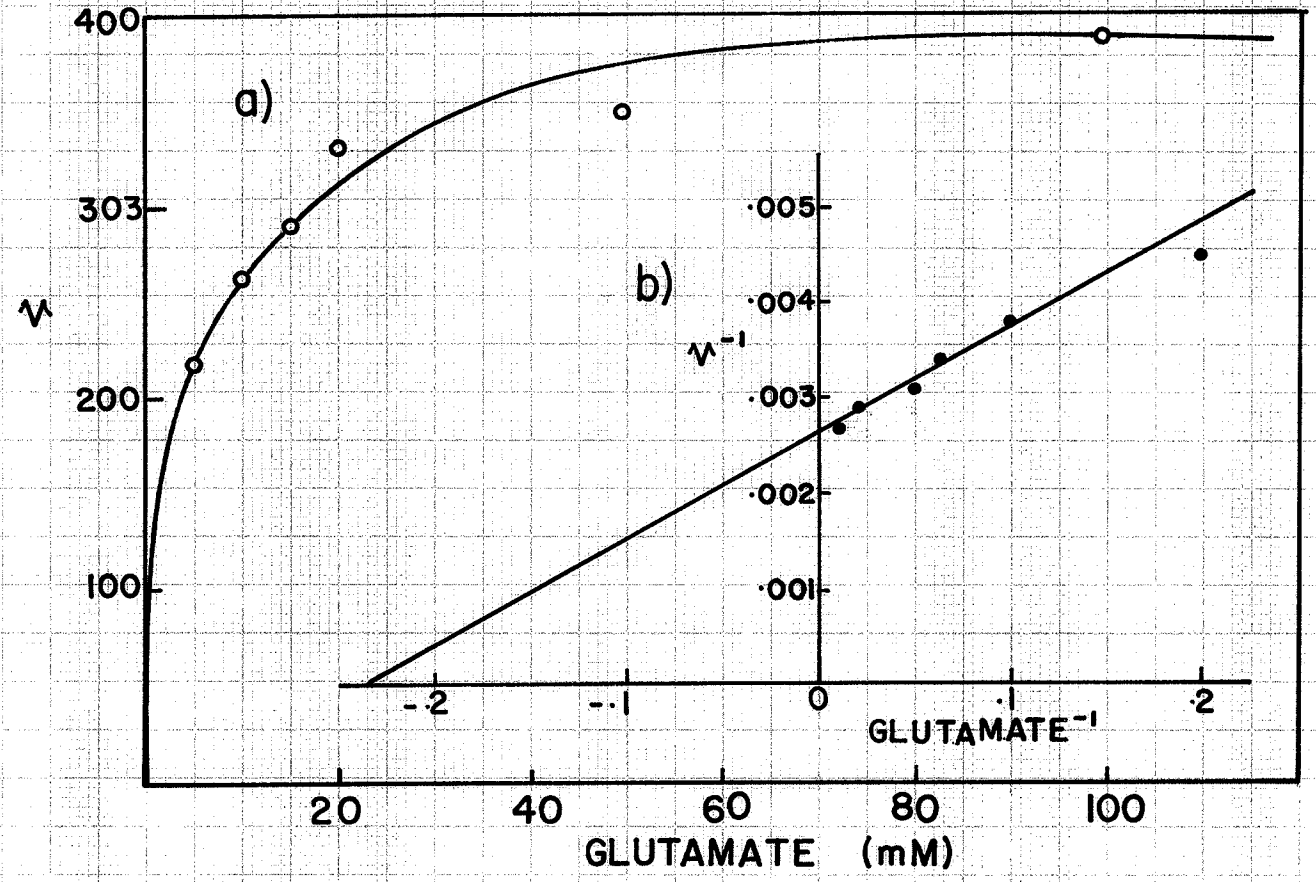
400
303
200
100
v
a)
b)
·005
·004
·003
·002
·001
v⁻¹
-·2
-·1
0
·1
·2
GLUTAMATE⁻¹
20
40
60
80
100
GLUTAMATE (mM)

Fig. 23. Initial velocity studies on glutamine synthetase from *B. emersonii*.

a) Rate concentration plot of enzyme rate against ATP concentration. The reaction system contained 125 mM NH_2OH, 25 mM Mn^{++}, 125 mM glutamate, 2.5 mM Cleland's reagent, 25 mM Imidazole buffer, pH 7.1, ATP as indicated, and 100 µl enzyme preparation.

b) Double reciprocal plots of data reported in Fig. 23a.

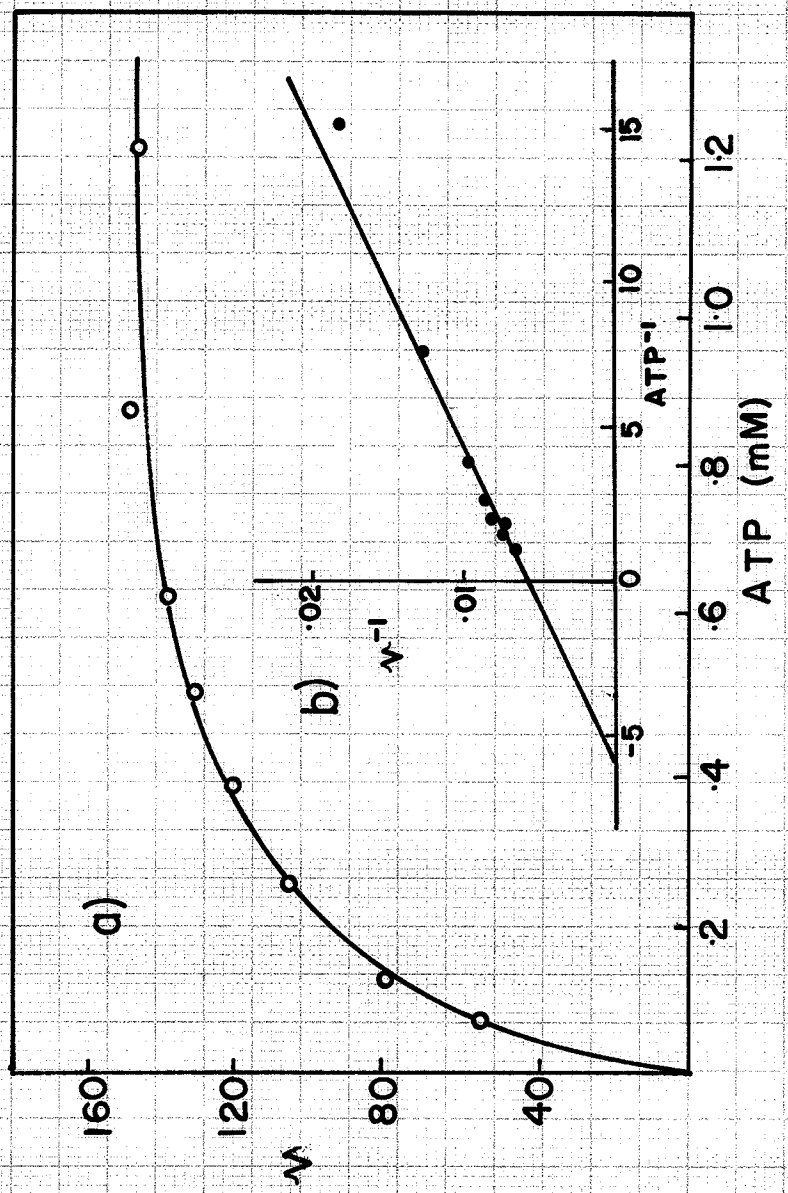
a)
b)
v
160
120
80
40
.2
.4
.6
.8
1.0
1.2
ATP (mM)
-5
0
5
10
15
ATP⁻¹
.01
.02
v⁻¹

Fig. 24. Initial velocity studies on glutamine synthetase from *B. emersonii*.

a) Rate concentration plot of enzyme rate against NH_2OH concentration. The reaction system contained 25 mM Mn^{++}, 125 mM glutamate, 2.5 mM Cleland's reagent, 25 mM Imidazole buffer, pH 7.1, 4.25 mM ATP, NH_2OH as indicated, and 100 µl of enzyme preparation.

b) Double reciprocal plot of data reported in Fig. 24a.

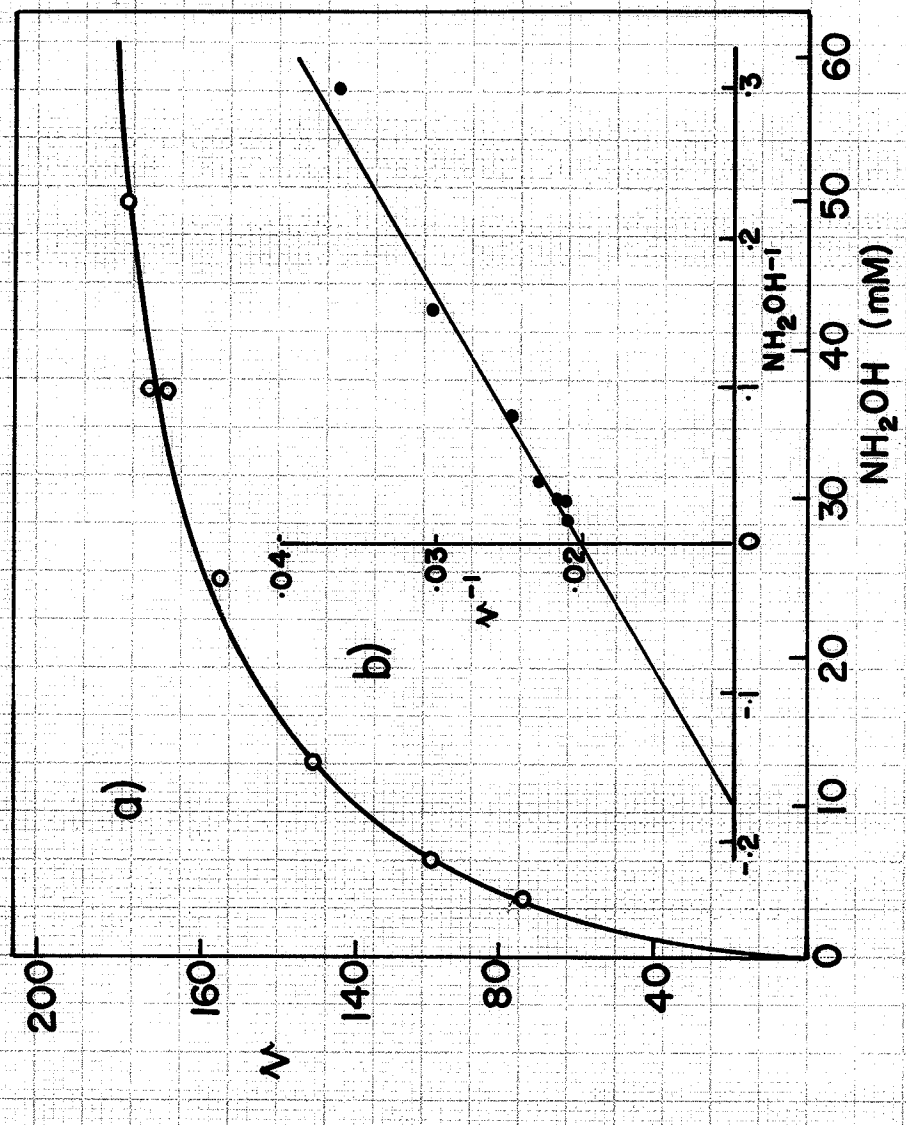
a)
b)
v
v^{-1}
NH_2OH (mM)
NH_2OH^{-1}
200
160
140
80
40
0
10
20
30
40
50
60
.04
.03
.02
-.2
-.1
0
.1
.2
.3

TABLE VIII

Kinetic Constants for Glutamine Synthetase from *B. emersonii*

Substrate	K_m
glutamate	4.4×10^{-3} M
NH_2OH	5.9×10^{-3} M
ATP	1.5×10^{-4} M

Fig. 25. The effect of Mn^{++} on the initial velocity of glutamine synthetase from B. emersonii. The reaction system contained 100 mM glutamine, 2.5 mM Cleland's reagent, 2.5 mM ATP, 100 mM NH_2OH, 25 mM Imidazole buffer, pH 7.1, Mn^{++} as indicated and 50 µl of enzyme preparation.

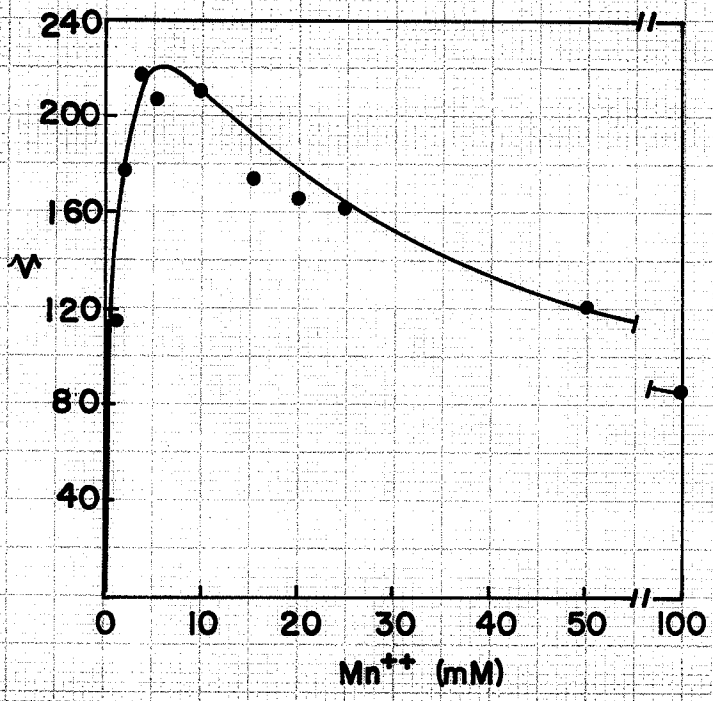

velocity is less than 40% of that at 5 mM Mn^{++}. Similar Mn^{++} inhibition has been observed on the glutamine synthetase from E. coli (Woolfolk and Stadtman, 1967).

Feedback Inhibition

Table IX records the results when the enzyme reaction proceeds in the presence of a number of potential effectors. Inhibition occurred with 6 of the inhibitors reported for glutamine synthetase from E. coli, namely, tryptophan, glycine, alanine, AMP, histidine, and CTP. Carbamyl phosphate showed no effect under the conditions of the assay, and GAP seemed to activate the enzyme. The apparent activating effect of glutamine will be discussed later. Other substances which showed inhibition were citrate, α-ketoglutarate, FDP, and GTP.

Further studies were done to find the relationships between five of the inhibitors, namely, histidine, alanine, glycine, AMP, and CTP, (Table X). Cumulative inhibition was observed between AMP, CTP, and any one of the amino acids. The amino acids, however, showed strong antagonistic effects toward each other. These judgements were made in the following manner. When inhibition by two effectors falls far below the prediction for cumulative inhibition, so that actual inhibition is in the range of the effect of one of the inhibitors alone, the inhibition is judged antagonistic. Predictions for cumulative inhibition are made as follows. If histidine alone inhibits 45% and alanine alone, 25%, the predicted cumulative effect is 45 + .25 (100-45) = 59%. If histidine and alanine were acting on separate isoenzymes, the effect would be

TABLE IX

Inhibition of Glutamine Synthetase

Inhibitor	Concentration	Percent Activity
Tryptophan	10 mM	96
Glycine	10 mM	96
Alanine	10 mM	92
AMP	10 mM	33
Histidine	10 mM	75
CTP	5 mM	56
GAP	10 mM	146
C.P.	10 mM	100
Glutamine	10 mM	123
Ornithine	10 mM	100
Citruline	10 mM	110
Arginine	10 mM	113
Citrate	10 mM	75
Isocitrate	10 mM	100
α-ketoglutarate	10 mM	75
FDP	10 mM	85
G6P	10 mM	100
GTP	10 mM	62
GDP	10 mM	100

The reaction system contained 10 mM glutamate, 2.5 mM Cleland's reagent, 2.5 mM ATP, 10 mM NH_2OH, 25 mM Imidazole buffer, pH 7.1, 10 mM Mn^{++}, and 50 µl of enzyme preparation.

TABLE X

Interactions Between Inhibitors of Glutamine Synthetase from *B. emersonii*

	Alanine		Glycine		AMP	
Histidine	45	25	45	20	45	65
	31	59	13	56	82	81
CTP	44	8	44	6	44	62
	52	51	48	48	77	78
AMP	62	8	65	20		
	67	65	73	72		
Glycine	20	25				
	9	40				

The reaction system contained 10 mM glutamate, 2.5 mM Cleland's reagent, 2.5 mM ATP, 10 mM NH_2OH, 25 mM Imidazole buffer, pH 7.1, 10 mM Mn^{++}, 50 µl enzyme preparation, and 10 mM of each inhibitor. The numbers in each box are expressed as percent inhibition with placement as follows:

1. upper left - effect of inhibitor to the left alone.
2. upper right - effect of inhibitor on top alone.
3. lower left - combined effect of both inhibitors.
4. lower right - predicted combined effect assuming cumulative inhibition.

additive, i.e., 45 + 25 = 70%.

DISCUSSION

I. A Kinetic Mechanism for $NADP^+$ specific Isocitrate Dehydrogenase

The oxidative decarboxylation of isocitrate involves the addition to the enzyme of two substrates and the release of three products. From initial reaction rate and product inhibition studies, the order of substrate addition and product release could be determined using procedures developed by Cleland (1963). Applying King and Attman (1956) determinant manipulations, a steady state rate equation for the reaction can be obtained.

If it is found from initial velocity studies that the double reciprocal rate-concentration plots are parallel when one substrate is varied, it implies, (according to Cleland) that the substrates are not added sequentially to the enzyme. The conclusion is that a product(s) is released before the addition of the second substrate. This type of mechanism is termed "ping pong".

Examination of Table III leads to the proposal of the following mechanism, presented in Cleland's graphical manner (1963):

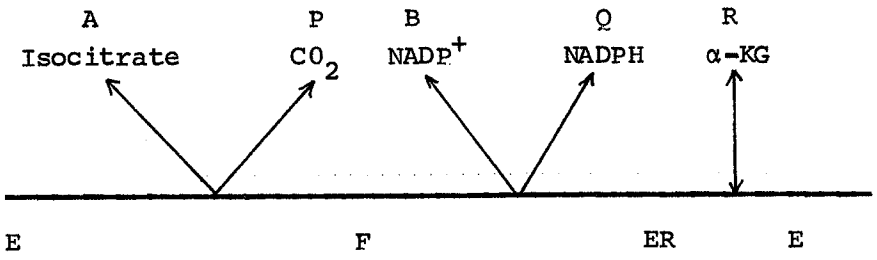

This reaction sequence could be termed Uni-Uni-Uni-Bi Ping Pong (Cleland, 1963). The decarboxylation of isocitrate and the reduction of $NADP^+$ are presented as Theorell-Chance reactions, with no kinetically detectable enzyme-substrate complex existing between the addition of substrate and

the release of product (Theorell and Chance, 1951). Schematically, the reaction could be represented as follows:

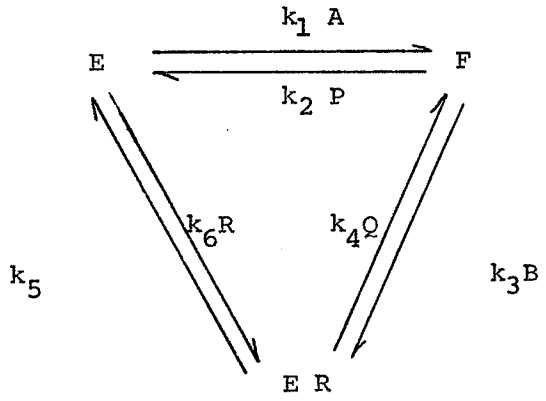

Using the method of King and Altman (1956) the following rate equation may be derived for the reaction:

$$v = \frac{V_1 \left(AB - \frac{PQR}{Keq}\right)}{K_bA + K_aB + \frac{K_qK_aK_bP}{KiqK_p} + AB + \frac{K_rK_aK_bQP}{KirKiqK_p} + \frac{K_aK_bRQ}{KirKiq} + \frac{K_aRB}{Kir} + \frac{K_bAQ}{Kiq} + \frac{K_gK_aK_bPR}{KirKiqK_p}}$$

If it is assumed that no product appears in initial velocity studies, terms containing P, Q or R may be deleted, to yield the equation below. The constants have been omitted for ease of manipulation and the equation has been linearized by inversion and rearranged into the slope-intercept form:

$$\frac{1}{v} = \frac{1}{V_1}\left[\frac{1}{B} + 1\right] + \frac{1}{V_1}\left[\frac{1}{A}\right] \quad \text{or} \quad \frac{1}{v} = \frac{1}{V_1}\left[\frac{1}{A} + 1\right] + \frac{1}{V_1}\left[\frac{1}{B}\right]$$

It can be seen that changes in A or B, when the other substrate is varied affect only the intercept of the lines, resulting in sets of parallel lines. With R as inhibitor the equation, when expressed as above, becomes:

$$\frac{1}{v} = \frac{1}{V_1}\left[\frac{1}{B} + 1\right] + \frac{1}{V_1}\left[1 + R\right]\frac{1}{A} \quad \text{or} \quad \frac{1}{v} = \frac{1}{V_1}\left[\frac{1}{A} + 1 + \frac{R}{A}\right] + \frac{1}{V_1}\left[\frac{1}{B}\right]$$

It is obvious that R affects only the slope when A is the variable substrate, and only the intercept when B is the variable substrate and A is unsaturating. When A is saturating, R should have no effect on the velocity of the reaction. This data corresponds exactly with experimental results when A = isocitrate, B = $NADP^+$, and R = α-ketoglutarate.

With Q as inhibitor, the equation may be written:

$$\frac{1}{v} = \frac{1}{V_1}\left[\frac{1}{B} + 1 + \frac{Q}{B}\right] + \frac{1}{V_1}\left[\frac{1}{A}\right] \quad \text{or} \quad \frac{1}{v} = \frac{1}{V_1}\left[\frac{1}{A} + 1\right] + \frac{1}{V_1}\left[1 + Q \quad \frac{1}{B}\right]$$

Q affects only the intercept when A is the variable substrate and B is unsaturating, and has no effect when B is saturating. When B is the variable substrate Q affects only the slope. Correspondence is again obtained when A = isocitrate, B = $NADP^+$ and Q = NADPH.

With P as inhibitor, the equation becomes:

$$\frac{1}{v} = \frac{1}{V_1}\left[\frac{1}{B} + 1\right] + \frac{1}{V_1}\left[1 + \frac{P}{B}\right]\frac{1}{A} \quad \text{or} \quad \frac{1}{v} = \frac{1}{V_1}\left[\frac{1}{A} + 1\right] + \frac{1}{V_1}\left[1 + \frac{P}{A}\right]\frac{1}{B}$$

The presence of P should affect only the slope when A or B is the variable substrate and should have no effect when the fixed substrate approaches saturation. If the preceding discussion is valid, P should correspond to carbon dioxide. In fact, concentrations of bicarbonate comparable with concentrations of the other inhibitors used have no significant inhibitory effect. When concentrations of bicarbonate up to one-hundred fold of the other inhibitors are used, inhibition is obtained. When isocitrate is the variable substrate this inhibition is competitive, as would be expected in this mechanism if $NADP^+$ were unsaturating. When $NADP^+$ is the variable substrate, extremely high concentrations of bicarbonate inhibit in a non-competitive manner. The latter result is not compatible with the mechanism proposed. The reasons for this less than perfect fit of bicarbon-

ate into the scheme may be due to one or more of the following factors: 1) Bicarbonate may not be a true substrate for the reaction (Siebert et al, 1957); 2) High concentrations of bicarbonate may affect the ionic environment of the enzyme and interfere with normal intermediate complex formation; 3) There may be an association between bicarbonate and magnesium which affects initial velocity patterns by effectively reducing the concentration of the cofactor.

In general there is good agreement between the predicted patterns and the experimental results. With few reservations it may be concluded that the proposed mechanism is correct. These reservations may be summarized as follows:

1) The proposed mechanism is only considered valid for the conditions under which the assays were conducted with respect to pH, ionic environment, temperature, the presence or absence of effectors, and in the narrow range of substrate concentrations used.

2) The in vivo mechanism may differ from the proposed theory.

3) The mechanism is unorthodox in that it allows decarboxylation to precede reduction. Instead of oxalosuccinate as the intermediate, as is usually assumed, the mechanism would necessitate the formation of hydroxyglutarate. Also, decarboxylation and reduction are separate sequential events in the proposed mechanism. Though unorthodox, this interpretation is credible when one considers the evolution of the catalytic capacity of the enzyme. It would seen to be more likely that one enzyme should develop two separate capacities independantly than that two capacities should be developed in concert.

II. The Regulation of $NADP^+$ and NAD^+ specific Isocitrate Dehydrogenase

It is the purpose of this section to compare the regulatory features of the $NADP^+$ specific IDH with those of the NAD^+ specific IDH from Blastocladiella. Their probable physiological roles can then be discussed in a later section.

pH Effects

The extreme sensitivity of the NAD^+ specific IDH to changes in pH has been reported and related to its mitochondrial role (LeJohn et al, 1969a). These studies show that the $NADP^+$ specificIDH is not very sensitive to pH changes (Fig. 1), which suggests that the enzyme may not be regulated by protons, and indicates that it may not be mitochondrial. This conclusion was supported by checking the $NADP^+$ specific IDH activity in a mitochondrial preparation from B. emersonii, obtained by the method of LeJohn, Jackson, Klassen and Sawula (1969). No significant activity was found.

Kinetic Mechanism

Although not intrinsically a regulatory feature, the kinetic mechanisms of the enzymes are strikingly different. The NAD^+ specific enzyme mechanism is "binary-ternary ordered" in the presence of activators, (LeJohn, 1969a), but the $NADP^+$ specific enzyme mechanism appears to be "Uni-Uni-Uni-Binary Ping Pong". This observation merely serves to suggest how basically different the two proteins might be, and allows for a theory of independent evolution for each.

Effectors

AMP, ADP, and citrate activate the NAD^+ specific IDH, while ATP and GTP inhibit it (LeJohn et al, 1969a). Experiments that were done to find

the effect of nucleotides on the $NADP^+$ specific IDH do not show the same patterns (Table IV and V). Inhibition is observed with the nucleotides ATP, ADP and AMP on the carboxylation and decarboxylation reactions and there is no differential effect between the nucleotides. While this may be bona fide inhibition, it could not be explained by the adenylate control hypothesis (Atkinson, 1966), and thus probably has no role in the regulation of energy flow. More work is needed to elucidate this effect, but one possible explanation is that inhibition may be due to chelation of Mg^{++} by the nucleotides. The inhibition by AMP makes this explanation improbable.

The effect of citrate on both reactions has been studied in more detail (Figs.14 and 15). Citrate inhibits the oxidation of isocitrate competively with respect of isocitrate, and inhibits the reduction of α-ketoglutarate. Again, the effect may be explained as a physiological control mechanism or an artifact due to chelation of Mg^{++} by citrate. The latter, however, is unlikely because of the different responses shown by isocitrate and α-ketoglutarate.

Reversibility

The reversal of the NAD^+ specific IDH has not been observed (LeJohn et al, 1969a). The $NADP^+$ specific IDH is readily reversible and studies on the reductive carboxylation of α-ketoglutarate suggest that this reaction may be of regulatory significance. It was found that NADPH was cooperative in initial velocity studies (Fig. 11). When α-ketoglutarate was the variable substrate, the double reciprocal rate concentration plots appear to be biphasic, suggesting a negative cooperative response (Fig. 12). When this experiment was repeated using Mn^{++} as the cofactor instead of Mg^{++}, however, positive cooperativity was observed (Fig. 13). Further work is necessary to see whether α-ketoglutarate cooperativity is actually a function of

the cofactor or something more complex. The conclusion that can be drawn at this time is that, since cooperative patterns are observed with the "reverse" reaction and not with the "forward" reaction, it is likely that the "reverse" is of physiological significance.

Ionic Strength

Table VI indicates that the $NADP^+$ specific IDH is not affected by an eight fold variation in ionic strength. On the other hand, Fig. 18 shows the dramatic inhibitory effect of an increase in ionic strength on the NAD^+ specific IDH in the absence of activators.

To investigate the nature of ionic inhibition of NAD^+ specific IDH, initial velocity were repeated in the absence of activators, since it is apparent from Fig. 18 that saturating effector concentrations can mask the effects of ionic strength.

Complex patterns of cooperativity emerged from these studies (Figs. 16 and 17). The obvious inflection of the double reciprocal plot for NAD^+ as the variable substrate indicated that a change in NAD^+ interaction had occurred at approximately 0.3 mM.

This observed change in interaction led to a different and more useful treatment of the data. Changeux (1963) and Atkinson *et al* (1965) have shown that the interaction of ligand binding sites may be analysed in terms of *n*, the slope of the line obtained when $\log \frac{v}{V_{max} - v}$ is plotted against $\log [S]$, where *v* is the enzyme velocity at the conditions stated, V_{max} is the maximal velocity of the enzyme at the concentration of fixed substrate or effector in question, and S is the variable substrate. The interaction coefficient, *n*, is a function of the number of substrate binding sites and of the strength

of interaction. For n to be a true index of interaction, the allosteric constant would have to approach infinity. In this discussion, since the allosteric constant is not known, n will be used only to assess relative changes in interaction, and no attempts will be made to assess the number of binding sites or to determine quantitative binding parameters.

Fig. 26 is an attempt to summarize the possibilities for ligand interactions in the form of theoretical curves. The allosteric constant is assumed to be infinitely large and the curves are only approximations of the functions they represent.

The interpretation of the data presented in Figs. 16-21 is greatly simplified by considering it in the light of what is known about the association-dissociation equilibrium of the enzyme. The NAD^+ specific IDH from Blastocladiella is known to have a monomeric molecular weight of 110,000 ± 10,000 daltons and the ability to aggregate to polymers of 500,000 daltons or more (LeJohn et al, 1969a). The aggregated enzyme is somewhat inactive relative to the activity of the monomer. The effector citrate, and the substrate isocitrate, are capable of dissociating the polymer whereas the effector AMP, and the substrate NAD^+, are not competent (LeJohn et al, 1969a). It is also known that increase in anionic strength favors polymerization (LeJohn et al, 1969b). It is clear, then, that effectors and substrates affect two equilibria, that between polymer and monomer, and that between active (R) and inactive (T) states:

$$\text{Polymer} \rightleftharpoons T \rightleftharpoons R$$

The changes of slope in the Hill plots reflect displacement of these equilibria. For example, increasing slope means that the inactive states are being favoured.

The effect of isocitrate can be seen in Figs. 16 and 17. As isocitrate increases

Fig. 26

The Modes of Ligand Interaction

1. Three basic possibilities:

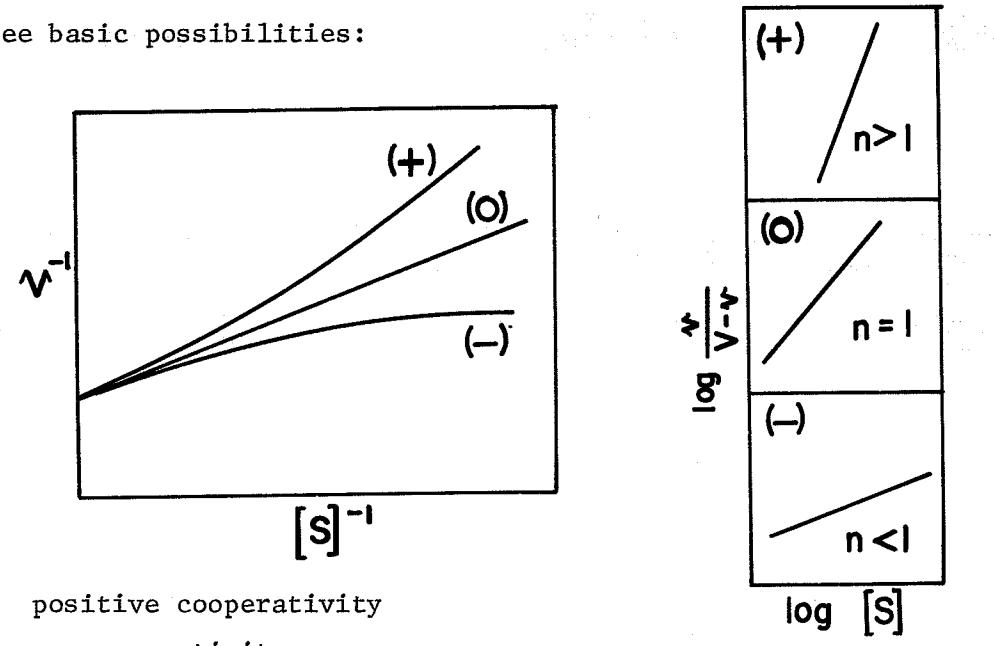

(+) positive cooperativity

(o) no cooperativity

(-) negative cooperativity

2. Mixed Cooperativity

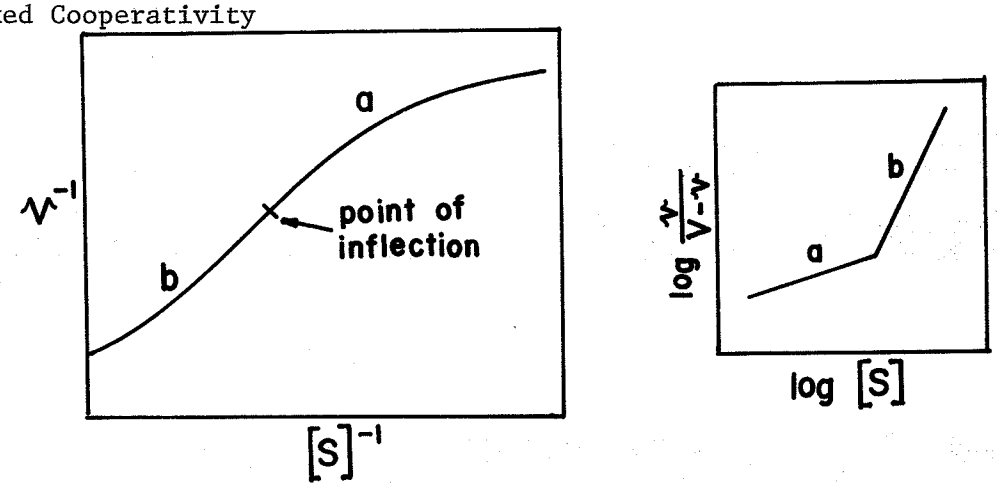

(Fig. 16) there is a decrease of slope, indicating that the R state is favoured. The same effect is observed in Fig. 17 where at high NAD^+ concentrations, the slope again decreases with increasing isocitrate. We may conclude from this that isocitrate is a good depolymerizing agent and that it maintains the monomer R $\rightleftharpoons$ T equilibrium efficiently.

Fig. 17 shows that as the NAD^+ concentration increases there is a sudden increase of slope. This could be interpreted to mean that at low NAD^+ concentrations, NAD^+ binds to the polymer but does not dissociate it. Instead, NAD^+ binding distorts the enzyme and induces negative or pseudo-negative cooperative effects on the enzyme.

The effects on these patterns of varying the anionic strength may be seen in Figs. 19 and 20. As ionic strength increases when isocitrate is varied, the slope increases, indicating that ionic strength favors the inactive (T) state (Fig. 19). At high NAD^+ concentrations, when NAD^+ is varied, the same effect is observed (Fig. 20).

When the effect of low activator concentrations on enzyme velocity was studied, it was found that citrate activation resembled the effect of NAD^+ in that it too could induce negative cooperative effects at low concentrations (Fig. 21), whereas AMP could not. Increased ionic strength increased the slope of the AMP plots, and high citrate had the same effect on the citrate plots. In each case, then, increasing ionic strength favors the less active states.

The foregoing may be summed up as follows:

$$\begin{array}{ccccc} & [M] & & [M] & \\ & [S] & & [S] & \\ \text{Polymer} & \rightleftharpoons & \text{T} & \rightleftharpoons & \text{R} \\ & \Gamma/2 & & \Gamma/2 & \end{array}$$

[M] = modifier (AMP, citrate)
[S] = substrate (Mn^{++}, isocitrate, NAD^+)

III. Glutamine Synthetase Inhibition

The results obtained in this study are only preliminary indications of the characteristics of glutamine synthetase from B. emersonii, and it would be premature to propose a medel for its control on the basis of this data. Certain conclusions, however, may be drawn:

1. B. emersonii glutamine synthetase shows cumulative feedback inhibition by a number of end products of the metabolic link but the pattern of inhibition is different from that observed for E. coli.

2. Interactions between inhibitors were observed, similar to those observed in glutamine synthetase from Bacillus lichenformis (Hubbard and Stadtman, 1967b) and contrary to the complete independance of inhibitors reported for E. coli enzyme (Woolfolk and Stadtman, 1964 and 1967a). Antagonistic interactions between glycine, alanine and histidine, as reported for B. lichenformis enzyme, parallel those found in B. emersonii. Synergism between AMP and histidine, as reported for B. lichenformis enzyme did not seem to occur for B. emersonii enzyme.

3. Other inhibitors, FDP, GTP, citrate and α-ketoglutarate, reported in Table IX, may have special significance in the physiology of B. emersonii. This will be discussed in the next section.

IV. Physiological Relationships

The proposed physiological role of the NAD^+ specific IDH-GDH enzyme complex associated with the mitochondrion has been discussed in Section III

of the "Historical". The results of this investigation can now be used to extend the existing theory.

It is clear that the $NADP^+$ specific IDH does not participate significantly in the control of energy flow since it is not differentially regulated by AMP and ATP, and does not appear to be an integral part of the citric acid cycle. If it is inhibited by citrate, as this report suggests, its activity should decrease under conditions when the NAD^+ specific IDH would be activated. This inverse regulation of the two isocitrate dehydrogenases could be viewed as a unidirectional valve, analogous to the unidirectional inhibition of GDH by citric acid cycle intermediates. It prevents return leakage of intermediates during active energy production.

Under conditions of citric acid cycle inhibition, the flow of carbon for the biosynthetic needs of the cell must still be kept up. It is becoming certain that the citric acid cycle in B. emersonii is incomplete, lacking α-ketoglutarate dehydrogenase (LeJohn, 1968; Khouw and McCurdy, 1969). In the absence of this step, carbon must flow to malate and oxaloacetate by way of the glyoxalate route. The only path by which carbon could re-enter the citric acid cycle from glutamate would then be the reverse reaction of the $NADP^+$ specific IDH, since the NAD^+ specific IDH is seemingly irreversible. This speculation is confirmed by the finding of cooperative kinetics for the reverse reaction of the $NADP^+$ specific enzyme, which make a regulatory role for this reaction credible. In general, then, NAD^+ specific IDH is concerned with the regulation of energy flow and its activation results in the ultimate accumulation of glutamate in a "glutamate sink". The $NADP^+$ specific IDH on the other hand, operates to maintain carbon flow, particularly the flow of glutamate back into the citric acid cycle.

The functions proposed for this enzyme in other organisms (see Section II of the "Historical") are not excluded by the above conclusions. The enzyme may be a valuable source of NADPH for biosynthetic purposes when catalysing the oxidative decarboxylation of isocitrate. It may also participate in respiration via the transhydrogenase route and so maintain a minimal energy turnover during citric acid cycle inhibition.

In seeking to correlate the modulation of glutamine synthetase with that of the two isocitrate dehydrogenases and GDH, the following findings are pertinent.

1. AMP is the most potent inhibitor of glutamine synthetase.
2. Citrate and α-ketoglutarate inhibit the enzyme.

According to the foregoing theory of IDH and GDH action, large quantities of glutamate would accumulate during periods of intense energy production. These periods would correspond to high citrate, AMP and α-ketoglutarate concentration in the cell. It is possible that under these conditions, excess glutamate could overpower the modulation of glutamine synthetase, and flood the pathways branching from glutamine, altering the levels of intermediates beyond the tolerance of the cell. Inhibition by metabolites and AMP could act to reinforce end-product inhibition on glutamine synthetase and thus ensure appropriate enzyme activity in spite of high glutamate levels. It is also possible that the inhibition of glutamine synthetase by citrate and α-ketoglutarate is a built-in device that acts to divert glutamate to other metabolic processes.

REFERENCES

Adair, G.S., J. Biol. Chem., 63, 529, 1925.

Atkinson, D.E., Ann. Rev. Biochem., 35, 85, 1966.

Atkinson, D.E., Hathaway, J.A. and Smith, E.C., J. Biol. Chem., 240, 2682, 1965.

Bernofsky, C., and Utter, M.F., J. Biol. Chem., 241, 5461, 1966.

Bernofsky, C., and Utter, M.F., Science, 159, 1362, 1968

Bohr, C., Zentr. Physiol. 17, 682, 1903.

Cantino, E.C., Lovett, J.S., Advance Morphogenesis, 3, 33, 1964.

Cantino, E.C., Truesdell, L.C., and Shaw, D.S., J. Elisha Mitchell Sci. Soc., 84, 125, 1968.

Changeux, J-P., Cold Spring Harbor Symp. Quant. Biol., 26, 497, 1963.

Changeux, J-P., Cold Spring Harbor Symp. Quant. Biol., 28, 497, 1963

Chen, R.F. and Plaut, G.W.E., Biochemistry, 2, 1023, 1963.

Cleland, W.W., Biochem. Biophys. Acta, 67, 104, 173, 188, 1963.

Elliott, W.H., Biochem. J., 49, 106, 1951.

Elliott, W.H., J. Biol. Chem., 201, 661, 1953.

Elliott, W.H., and Gale, E.F., Nature, 161, 129, 1948.

Ernster, L. and Navazio, F., Exptl. Cell Research, 11, 483, 1956.

Ernster, L., and Navazio, F., Biochim. Biophys. Acta, 26, 408, 1957.

Florini, J.R., and Vestling, C.S., Biochim. Biophys. Acta, 25, 575, 1957.

Goebell, H., and Klingenberg, M., Biochem. Z., 340, 441, 1964.

Greville, G.D. Intracellular Compartmentation and the Citric Acid Cycle. In Citric Acid Cycle, Lowenstein, J.M. (ed.), Marcel Dekker, New York, p.1-136.

Hansen, R.S., and MacKechnie, I., Biochem. Biophys. Res. Commun., 36, 300, 1969.

Hubbard, J.S., and Stadtman, E.R., J. Bacteriol., 93, 1045, 1967.

Hubbard, J.S., and Stadtman, E.R., J. Bacteriol., 94, 1016, 1967.

Jackson, Susan, M.Sc. Thesis, University of Manitoba, 1969.

Kaplan, N.O., Swartz, M.N., Frech, M.E., and Ciotti, M.M., Proc. Natl. Acad. Sci., 42, 481, 1956.

Khouw, B.T., and McCurdy, H.D., J. Bacteriol., 99, 197, 1969.

King, E.L., and Altman, C., J. Phys. Chem., 60, 1375, 1956.

Kingdon, H.S., Shapiro, B.M., and Stadtman, E.R., Proc. Natl. Acad. Sci., 58, 1703, 1967.

Kohlhaw, G., Dragart, W., and Holzer, H., Biochem. Z., 341, 224, 1965.

Kornberg, A., and Pricer, W.E., Jr., J. Biol. Chem., 189, 123, 1951.

Koshland, D.E. Jr., and Neet, K.E., Ann. Rev. Biochem., 37, 359, 1968.

Koshland, D.E. Jr., Nemethy, G. and Filmer, D., Biochemistry, 5, 365, 1966.

Krebs, H.A., Biochem. J., 29, 1951, 1935.

LeJohn, H.B., Biochem. Biophys. Res. Commun., 32, 278, 1968.

LeJohn, H.B., J. Biol. Chem., 243, 5126, 1968.

LeJohn, H.B., and Jackson, Susan, J. Biol. Chem., 243, 3447, 1968.

LeJohn, H.B., and Jackson, Susan, Biochem. Biophys. Res. Commun., 33, 613, 1968.

LeJohn, H.B., Jackson, Susan, Klassen, G.R., and Sawula, R.V., J. Biol. Chem., In-press, 1969.

LeJohn, H.B., Klassen, G.R., and Yen, F.S., In-preparation, 1969.

LeJohn, H.B., McCrea, Barbara E., Suzuki, I., Jackson, Susan, J. Biol. Chem., 244, 2484, 1969.

Leuthardt, F., and Bujard, E., Helv. Med. Acta, 14, 274, 1947.

Lineweaver, H., and Burk, D., J. Am. Chem. Soc., 56, 658, 1934.

Lowry, O.H., Rosebrough, N.J., Farr, A.L., and Randall, R.J., J. Biol. Chem., 193, 265, 1951.

Lovett, J.S., J. Bacteriol. 96, 962, 1968.

Marr, J.J., and Weber, M.M., J. Biol. Chem., 243, 4973, 1968.

Marr, J.J., and Weber, M.M., Biochem. Biophys. Res. Commun., 34, 12, 1969.

McCrea, B.E., M.Sc. Thesis, University of Manitoba, 1969.

Monod, J., Wyman, J., and Changeux, J-P, J. Mol. Biol., 12, 88, 1965.

Moyle, J. and Dixon, M., Biochem. J., 63, 548, 1956.

Ochoa, S., and Weisz-Tabori, E., J. Biol. Chem., 174, 123, 1948.

Orstrom, A., Orstrom, M., Krebs, H.A., and Eggleston, L.V., Biochem. J., 33, 995, 1939.

Ozaki, H., and Shiio, I., J. Biochem., 64, 355, 1968.

Plaut, G.W.E. 1963. Isocitrate Dehydrogenases. p.105-126. In The Enzymes, Boyer, P.D., Lardy, H., Myrback, K. ed. vol. 6.

Plaut, G.W.E., and Sung, S.C., J. Biol. Chem., 207, 305, 1954.

Purvis, J.L., Biochim. Biophys. Acta, 30, 440, 1958.

Rall, T.W., and Sutherland, E.W., Cold Spring Harbor Symp. Quant. Biol., 26, 347, 1961.

Ravel, J.M., Humphreys, J.S., and Shive, W., Arch. Biochem. Biophys., 111, 720, 1965.

Salganicoff, J., and Koeppe, R.E., J. Biol. Chem., 243, 3416, 1968.

Sanwal, B.D., Stachow, C.S., and Cook, R.A., Biochemistry, 4, 410, 1965.

Shiio, I., and Ozaki, H., J. Biochem., 64, 45,1968.

Shapiro, B.M., and Stadtman, E.R., J. Biol. Chem., 243, 5069, 1967.

Siebert, G., Dubuc, J., Warner, R.C., and Plaut, G.W.E., J. Biol. Chem., 226, 965, 1957.

Speck, J.F., J. Biol. Chem., 179, 1387, 1949.

Stadtman, E.R., Bacteriol. Rev., 27, 170, 1963.

Stein, A.M., Kaplan, N.O., and Ciotti, M.M., J. Biol. Chem., 234, 979, 1959.

Stein, A.M., Stein, J.H., and Kirkman, S.K., Biochemistry, 6, 1370, 1967.

Sung, S.C., and Hsu, C.H., Formosan Med. Assoc., 56, 103, 1957.

Theorell, H., and Chance, B., Acta Chem. Scand., 5, 1127, 1951.

Valentine, R.C., Shapiro, B.M., and Stadtman, E.R., Biochemistry, 7, 2143 1968.

Woolfolk, C.A., Shapiro, B., Stadtman, E.R., Arch. Biochem. Biophys., 116 177, 1966

Woolfolk, C.A., and Stadtman, E.R., Biophys. Biochem. Res. Commun., 17, 313, 1964.

Woolfolk, C.A., and Stadtman, E.R., Arch. Biochem. Biophys., 118, 736, 1967.